2-B
MIT

303

MSC Internal Note 65-EG-33

no

Project Apollo

Simulation Study of Manual Control Techniques for Lunar Orbit Rendezvous

Prepared by: Ronald W. Simpson
Ronald W. Simpson, G&CD

Paul J. Stull
Paul J. Stull, G&CD

Ronald L. Wyrick
Ronald L. Wyrick, G&CD

James R. Brickel
James R. Brickel, FCSD

James R Brickel for
Dean F. Grimm, FCSD

Herbert E. Smith
Herbert E. Smith, G&CD

Approved by: David C. Cheatham for
David W. Gilbert
Chief, Engineering Simulation Branch, G&CD

Floyd V Bennett for
Jack Funk
Chief, Theoretical Mechanics Branch, G&CD

R G Chilton
Robert G. Chilton
Deputy Chief, Guidance & Control Division

C. H. Woodling
For Warren J. North
Chief, Flight Crew Support Division

NATIONAL AERONAUTICS AND SPACE ADMINISTRATION
MANNED SPACECRAFT CENTER
Houston, Texas
August 2, 1965

N70-34344

SIMULATION STUDY OF MANUAL CONTROL TECHNIQUES FOR LUNAR ORBIT RENDEZVOUS

Ronald W. Simpson, et al

National Aeronautics and Space Administration
Washington, D. C.

2 August 1965

SUMMARY

A hybrid simulation of manual control of the terminal phase of lunar orbit rendezvous has been conducted. The rendezvous was simulated in six degrees of freedom using two analog computers, a fixed-base simulator, and a digital differential analyzer. The fixed-base simulator contained the pilot controls and instrument displays.

Rendezvous of the pilot controlled LEM spacecraft with an orbiting CSM spacecraft was performed from five typical LEM/CSM intercept and miss trajectories. Six different thrusting techniques were evaluated for each trajectory. The techniques differed with respect to the criteria used for LOS rate control and thrusting procedures. The quantities displayed to the pilot were relative range between the two spacecrafts, relative range-rate, LOS angles between the spacecrafts, and LOS angular rate.

From the point of view of ΔV expenditure, it was determined that thrusting along the vector sum of the required changes in relative range-rate and LOS angular rate was most efficient. Therefore, the most efficient technique is one where the thrusting is directed along this vector sum thereby controlling relative range-rate and LOS angular rate concurrently. This technique requires the pilot to use a nomogram to determine the required thrust vector angle with respect to the LOS.

The performance of the recommended manual thrusting technique was compared with that of the PNGS. This comparison indicated the manual technique requires about 30% more ΔV than the PNGS. Thrusting schedules for both the manual technique and the PNGS are recommended.

INTRODUCTION

Insuring the success of the LEM/CSM lunar orbit rendezvous maneuver requires that a manual rendezvous control technique be developed as a backup to the automatic primary guidance mode (PNGS). The ΔV requirement of the manual technique must be within the ΔV budgeted for the terminal rendezvous, and the thrust requirement for the maneuver must also be compatible with the LEM thrust capability.

A manual rendezvous-control technique has been developed by GAEC which satisfies the above requirements. Ideally, however, any backup technique should allow the pilot to monitor the primary mode of control, i.e., the criterion for transition from PNGS operation to manual takeover should be compatible with the criterion for monitoring the PNGS.

In view of the requirements imposed upon an acceptable manual backup rendezvous-control technique, the Guidance and Control Division conducted a simulation study to develop such a technique. The objectives of this simulation were (1) to develop a manual rendezvous-control technique which is efficient, compatible with the LEM systems and fuel budget, capable of monitoring PNGS operation, and requires only range, range rate, and LOS angle and rate information be displayed to the pilot and (2) to compare the ΔV performance of the manual technique referred to in objective (1) with the ΔV performance of GAEC's manual backup rendezvous technique and MIT's primary automatic guidance mode for terminal rendezvous.

SCOPE

This simulation covered only the terminal rendezvous portion of the LEM mission, which was assumed to occur between the ranges of 25 nautical miles (n.mi.) and 500 feet. Both intercept and miss trajectories were investigated for normal and abort rendezvous cases. The technique was based on the trajectories resulting from the concept of LEM rendezvous transfer at ascent burnout to a direct rendezvous (i.e., no parking orbit). Since this work was completed, newer rendezvous trajectory concepts have evolved. However, the terminal rendezvous methods developed in this simulation program still apply but with new initial conditions and a different range/range-rate profile.

SYMBOLS

(A, E)	Azimuth and elevation angles of the CSM with respect to the LEM body axis system, degrees
$[B]$	Euler angle transformation matrix from inertial to LEM body axis system
$[B]^{-1}$	Inverse of $[B]$.
(F_x, F_y, F_z)	Body translation thrusts transformed to the inertial axes, lb
g	Earth gravity, 32.2 ft/sec^2
G	Universal gravitation potential, 3.44×10^{-8} ft^4/lb-sec^4
$I_{sp}(RCS)$	Specific impulse of RCS jet fuel, sec
$I_{sp}(ASC)$	Specific impulse of ascent engine fuel, sec
(I_{xx}, I_{yy}, I_{zz})	Moments of inertia of LEM about its principal axes, slug-ft^2
(I_{xy}, I_{xz}, I_{yz})	Products of inertia of LEM, slug-ft^2
K_A	Attitude feedback gain
K_R	Rate feedback gain
K_S	Attitude controller gain
(l_q, l_r, l_p)	Attitude control moment arms, ft
l_z	Characteristic jet damping moment arm, $\lvert Z_{cg} - Z_{ASCXP} \rvert$, ft
m	Mass of LEM, slugs
M	Mass of moon, 5.02085×10^{21} slugs
(M_{cq}, M_{cr}, M_{cp})	Attitude control moments of LEM, ft-lb
(q, r, p)	LEM angular rates about its body axes, deg/sec
$\bar{r}_f$	Inertial position vector of LEM, ft
(r_{fx}, r_{fy}, r_{fz})	Components of $\bar{r}_f$, ft.

SYMBOLS (Continued)

$\bar{r}_s$	Inertial position vector of CSM, ft
$\bar{R}$	Range vector of LEM with respect to CSM, ft
S	Laplace operator
$(T_{1\ldots16})$	LEM RCS thrusters
T_{ASC}	Ascent engine thrust, lb
T_{RCS}	RCS thrust, lb
(T_x, T_y, T_z)	Total thrust along the LEM X_b, Y_b, Z_b axes, lb
ΔV	Characteristic velocity, ft/sec
X_{cg}	Location of LEM c.g. along the X_b axis, ft
(X_b, Y_b, Z_b)	LEM body axes
(X_B, Y_B, Z_B)	Components of $\bar{R}$ along the LEM body axes, ft
(X_I, Y_I, Z_I)	Components of $\bar{R}$ along the inertial axes, ft
$\bar{Y}_{cg}$	Location of LEM cg along the Y_b axis, ft
$\bar{Z}_{cg}$	Location of LEM cg along the Z_b axis, ft
Z_{pads}	Location of LEM leg pads along the Z_b axis, ft
Z_{RCS}	Location of LEM RCS jet plane along the Z_b axis, ft
Z_{ASC}	Location of LEM ascent engine attachment point, ft
Z_{ASCXP}	Location of LEM ascent engine exit plane, ft
ϵ	Error signal
$(\epsilon_\theta, \epsilon_\psi, \epsilon_\phi)$	Pitch, yaw, and roll error signals
$(\epsilon_{\theta_B}, \epsilon_{\psi_B}, \epsilon_{\phi_B})$	Pitch, yaw, and roll error signals transformed to the LEM body axes
(θ, ψ, ϕ)	Pitch, yaw, and roll angles, degrees

$(\theta_c, \psi_c, \phi_c)$	Pitch, yaw, and roll commanded angles, degrees
λ	Central angle to CSM measured from landing site, degrees
τ_1	Time delay of RCS jets, sec
τ_2	Time delay of reference attitude feedback signal, sec
ω	Angular velocity of the CSM local vertical, rad/sec

SUBSCRIPTS

o	Initial value
t	With resepct to time

One dot over a quantity denotes the first derivative with respect to time and two dots over a quantity denotes the second derivative with respect to time. An arrow over a quantity denotes a vector.

DESCRIPTION OF SIMULATION

General

The LEM and CSM were simulated in six and three degrees-of-freedom, respectively, using hybrid computer equipment coupled with a fixed-base simulator cockpit containing the pilot controls and instrument displays. A block diagram of the computer mechanization is shown in figure 1. The translation equations of motion of the LEM relative to the CSM were mechanized on a digital differential analyzer (DDA). A general purpose digital computer was utilized for inputs and outputs for the problem and for controlling the operational modes of the DDA.

The rotational equations of motion of the LEM relative to an inertial set of axes were mechanized on an analog computer. Another analog computer was used to continuously compute inertial-to-body and body-to-inertial transofrmations, which in turn, were used to compute target line-of-sight information. The analog computers received inertial position and velocity data from the DDA through digital to analog converters.

A virtual image optical display system was used to present an out-the-window display of the target to the pilot. Inertial velocity data were fed to the special purpose display digital computer to continuously update the target position. Control of the terminal rendezvous was maintained by the pilot through monitoring of the instrument and visual displays.

Equations of Motion

The relative motion of the LEM with respect to the CSM was expressed in six degrees-of-freedom and was represented by translation and rotation equations of motion which were derived for an inertial coordinate system centered in the moon as shown in figure 2. The moon model was considered to be spherical and nonrotational, which justifies the assumption of this coordinate system as an inertial set. The Z_I axis is directed positive away from the landing site (landing site vertical), the X_I axis is parallel to the landing site horizontal pointing west, and the Y_I axis completes the right-handed set. A detailed block diagram of the translation equations of motion are shown in figure 3.

The rotation equations of motion, as mechanized in the attitude control system, for the pitch, yaw, and roll axes are shown in figures 4, 5, and 6, respectively. The body axes are defined for the LEM in figure 7 and the Euler angle sequence used to reference the LEM body axes with respect to the inertial reference was θ, ψ, ϕ.

Simulator Cockpit Displays

Instrument displays were provided in the simulator cockpit and were driven by outputs from the computers. A layout of the instrument panel is shown in figure 8a. Figures 8b to 8d give details of the instrument displays. Range, range rate, and LOS angles and rates were provided for manual control.

Simulator Cockpit Controls

The attitude controller was a three-axis hand controller of the Gemini type as shown in figure 9. Maximum deflection of the attitude controller in any direction is 10 degrees. The controller is spring loaded so that if no force is applied, the handle returns to the upright position. Movements of the hand controller in the pitch direction are about a pivot joint located approximately halfway up the handle. Yaw maneuvers are performed by movement of the handle about the longitudinal axis of the handle. Roll maneuvers are performed by movements of the handle. The physical characteristics of the attitude controller are given below:

Maneuver	Break-out moment	Moment at maximum deflection
roll	3 in-lb	9 in-lb
pitch	5 in-lb	23 in-lb
yaw	6.5 in-lb	14 in-lb

The translation jet hand controller used in this simulation is shown in figure 10. Operating forces for X_b, Y_b, and Z_b translation jets are linear and have the following characteristics.

breakout forces - 1 1/4 to 1 3/4 lbs
full travel forces - 3 1/2 to 4 lbs

Translation and Attitude Control Systems

The translational control system was capable of operation only in direct mode. A thrust buildup and decay time constant of 15 milliseconds was used to simulate the actual reaction jet response.

Three modes of operation of the attitude control system were direct (D), rate-command (RC), or rate-command attitude-hold (RCAH). The jets were operated in on-off, minimum impulse, or pulse-ratio modulation thrust modes. These modes of operation were provided by a jet select logic and signal modulation box. The discussion below describes the operation of the D, RC, and RCAH modes:

D - The direct mode operates as an acceleration command system as the attitude jets fire continuously as long as the attitude stick is deflected beyond its dead zone. This switch is shown in figures 4, 5, and 6. The acceleration capability of the LEM about its X_b (roll), Y_{b_2} (pitch), and Z_b(yaw) axes during the rendezvous maneuver are $42.70^{\circ}/sec^2$, $24.65^{\circ}/sec^2$ and $21.00^{\circ}/sec^2$, respectively.

RC - In RC mode, the followup circuit switches, located in the attitude feedback loop, close so that the output angle (θ, ψ, or ϕ) is followed and θ, ψ, or ϕ cancel $-\theta_c$, $-\psi_c$, or $-\phi_c$ respectively, depending on whichever control circuit is in operation. Thus, body angular rate is the only feedback term. Rate gyro characteristics are simulated in the rate feedback loop. The maximum rate which can be commanded in all three axes is $20^{\circ}/sec$.

RCAH - When the attitude control stick is within the dead zone in all three axes, the followup switches in the attitude feedback loops of all three axes are opened. When the stick is out of the dead zone in any axis, the followup switches in all three axes close. In this mode, the followup circuit either follows the output angle with a 0.1 second time delay or holds the last value of the output angle. For zero rate command, θ_c (or ψ_c or ϕ_c) remains constant and becomes the attitude command signal.

<u>Characteristics of Simulated LEM</u> - The LEM simulated for the purpose of this study had the following characteristics:

m_o	=	159 slugs*	(initial)
I_{xx}	=	1476 slug ft^2	(constant)
I_{yy}	=	2557 slug ft^2	(constant)
I_{zz}	=	2724 slug ft^2	(constant)
I_{xy}	=	- 13 slug ft^2	(constant)
I_{yz}	=	- 44 slug ft^2	(constant)
I_{xz}	=	-173 slug ft^2	(constant)
$\bar{X}_{cg}$	=	0.0333 ft	(constant)
$\bar{Y}_{cg}$	=	0.0500 ft	(constant)
$\bar{Z}_{cg}$	=	0.000 ft	(constant)
Z_{pads}	=	+14.23 ft	(constant)
Z_{RCS}	=	0:00 ft	(constant)
Z_{ASC}	=	+1.75 ft	(constant)
Z_{ASCXP}	=	+4.67 ft	(constant)
M_{cp}	=	$\pm$1100 ft-lbs	(roll)
M_{cq}	=	$\pm$1100 ft-lb	(pitch)
M_{cr}	=	$\pm$1000 ft-lb	(yaw)
T_x	=	$\pm$200 lbs	
T_y	=	$\pm$200 lbs	
T_z	=	$\pm$200 lbs (4 jets can be used which will give a thrust of $\pm$400 lbs)	
T_{ASC}	=	3500 lbs	
I_{sp}(RCS)	=	275 sec	
I_{sp}9ASC)	=	306 sec	
*m_o	=	248 slugs for abort case.	

It was assumed that the rendezvous radar and its interface with the displays were functioning properly with a $\pm$ 0.2 mr/sec bias error in LOS rate. The LEM mass was updated using the equation given below:

$$
\begin{aligned}
m_t &= m_o - \int \dot{m}\,dt \\
&= m_o - \int \frac{|T_{ASC}|}{g I_{sp(ASC)}}\,dt - \frac{W_A}{g} - \frac{W_B}{g} \\
&= m_o - \frac{1}{g}\left[\int \frac{|T_{ASC}|}{I_{sp(ASC)}}\,dt + W_A + W_B\right] \\
&= m_o - 0.031055\left[\int \frac{|T_{ASC}|}{I_{sp(ASC)}}\,dt + W_A + W_B\right]
\end{aligned}
$$

W_A and W_B are defined in Appendix A.

MANUAL CONTROL TECHNIQUES

General

In total, six manual control techniques were evaluated. GAEC's technique, Technique No. 1, and Technique No. 4 are basically different techniques; Techniques No. 2 and 3 are modifications of Technique No. 1, and Technique No. 5 is a modification of Technique No. 4. GAEC's technique and Technique No. 1 were developed out of digital computer studies. Technique No. 4, however, was developed in this hybrid simulation. The theories underlying each of the three basic techniques are explained below along with definitions of each technique. The modifications which were made to the three basic techniques are also explained below (Techniques No. 2, 3, and 5); however, the reasons for these modifications are more easily explained under the section of this report titled, DISCUSSION OF TEST RESULTS.

<u>GAEC Technique</u> - This technique was designed to be compatible with the different transfer orbits presently planned for the LEM/CSM lunar orbit rendezvous. Both upper and lower boundaries are used in the terminal range-rate schedule. The upper boundary assures that the range-rate stays within the acceleration capability of the LEM RCS jets whereas the lower boundary assures an intercept. The inertial LOS angular rate is recurrently controlled to 0.4 milliradians per second to assure an efficient intercept. A sequential description of this technique is given in Appendix C.

<u>Technique No. 1</u> - The philosophy used in this technique is that an intercept course exists when the range-rate becomes stabilized in the negative direction. The range-rate is maintained in this stable condition by thrusting perpendicular to the LOS; i.e., by controlling the LOS rate. Thus, the criteria used to determine when a LOS correction is needed in this technique is different from that of the GAEC technique. However, when a LOS rate correction is made, the same thrusting procedure is used as in the GAEC technique. The range-rate schedule for this technique (see Appendix C) uses only an upper bound on range-rate at each range checkpoint.

<u>Technique No. 2</u> - This technique is identical to Technique No. 1 in method; however, the GAEC terminal rendezvous schedule was used for range and range-rate. A tighter control is maintained on LOS rate by controlling to 0.4 mr/sec rather than 1.0 mr/sec.

<u>Technique No. 3</u> - This technique is the same as Technique No. 2 except in the criteria used to determine when a LOS rate correction is needed. The LOS rate is reduced to 0.4 mr/sec upon a 10 fps drop in range-rate if the range-rate is above 100 fps or upon a 10% drop in range-rate if the range-rate is below 100 fps.

<u>Technique No. 4</u> - This technique is based on the fact that the most economical way to make ΔV inputs in different directions is to thrust along the vector sum of the required ΔV inputs. Thus, this technique commands thrust along the vector sum of the desired LOS rate and range-rate corrections. The elevation or azimuth angle required for this type of thrusting is obtained from the nomogram shown in figure 11. Controlling the spacecraft attitude to the required LOS angle is facilitated by marking elevation and azimuth angle scales on the FDAI error needles in increments of 30° (figure 12). LOS rate is given in units of feet/second so that the same nomogram can be used for the required correction at each range checkpoint. Thus, an approximate computation of the required LOS rate correction in feet/second must be made at each range checkpoint using the equation $\Delta V_{\dot{\epsilon}} = (R)\ (\Delta\dot{\epsilon} \times 10^{-3})$ fps. A detailed explanation of the steps involved in this manual control technique and the terminal range-range rate schedule used is given in Appendix C.

<u>Technique No. 5</u> - This technique uses the same philosophy as Technique No. 4. However, the nomogram used to obtain the thrust vector angle required for a combined correction of LOS angular rate and range-rate was modified to make the control task easier. This nomogram, as shown in figure 13, gives LOS angular rate in units of milliradians/second versus range rate in units of feet/second for each range checkpoint. The lowest value given on each LOS rate and range-rate scale are the values to which these parameters must be controlled at each range checkpoint. The pilotage procedure for using this nomogram for manual control of terminal rendezvous is given in Appendix C.

TEST PROGRAM

Test Cases

The five test cases used to evaluate the various manual rendezvous-control techniques were as follows:

(1) 180° intercept with an intercept velocity of 97 fps;

(2) Near 180° transfer with $3\frac{1}{2}$ n.m. miss;

(3) Near 180° transfer with 5 n.m. miss;

(4) Near 210° transfer ($\frac{1}{2}^{\circ}$ out-of-plane) with 6 n.m. miss;

(5) 230° intercept from an aborted powered descent occurring 365 seconds after initiation of the powered descent with an intercept velocity of 200 fps.

The initial conditions for these test cases are given in table 1. Variplotter recordings of coasting trajectories for these cases are shown in Appendix D.

Run Schedule

Three research pilots from the Flight Crew Support Division were used as test crews in this simulation. In total, approximately 175 runs were made, the majority of which were on cases (4) and (5). Runs were made both with and without LOS angular rate errors present in the pilot display of this quantity.

DISCUSSION OF TEST RESULTS

General

Evaluation of the different manual rendezvous-control techniques was primarily accomplished by determining the ΔV requirements of each technique for the different transfer orbits flown. In addition to evaluating the relative efficiency of each of the manual control techniques, digital computer runs were made for these same five transfer orbits using the PNGS to determine the efficiency of manual control techniques in general as compared to that of the PNGS for this maneuver. The average ΔV for the runs made for each condition obtained in this simulation are presented in table 2. Because of a time limitation, radar error and error-free runs were not made for every technique, and every transfer orbit. The test matrix used allowed the greatest number of techniques to be evaluated in as many conditions as possible in the time available. The PNGS digital studies contained no error sources and was therefore assumed to be operating perfectly. Typical range, range-rate plots obtained from data runs using Technique No. 5 are presented in Appendix E.

Effect of LOS Rate Control - The study revealed that to a certain point the ΔV requirements were reduced for any technique when a tighter control was maintained on the LOS rate. This explains the higher ΔV requirements for Technique No. 1 as compared to the GAEC Technique because the GAEC Technique controls the LOS rate to a value which is 0.6 mr/sec lower than that of Technique No. 1. Technique No. 2 allowed the LOS rate to be controlled to the same value as in the GAEC Technique; however, because of the criteria for making LOS rate corrections in Technique No. 2, a fewer number of corrections are made. Thus, the ΔV requirements for Technique No. 2 were still higher than the GAEC Technique. Technique No. 3 involved a change in the criteria used to determine when a LOS rate correction was required. This change resulted in more LOS rate corrections and, thus a lower ΔV comparable to that of the GAEC Technique. It should be pointed out that the main effect of using the GAEC range-rate schedule in Techniques No. 2 and 3 was to maintain the range-rate at a higher value throughout the run which resulted in shorter run times. The effect of over-controlling the LOS rate was determined when runs were made using Technique No. 4 in conjunction with radar errors. It can be seen in table 2 that for this technique with radar LOS rate errors in the plus direction, attempted rendezvous for the $3\frac{1}{2}$ and 5 nautical mile miss cases were unsuccessful. This is because these two transfers have LOS rates in the positive direction, and as the 0.2 mr/sec error in the indicated value of this quantity was also in the positive direction, the LOS rate

was controlled to a true rate of +.05 mr/sec instead of +0.25 mr/sec as called for by the procedure. Technique No. 5 prevented aborts from occurring on these two cases by using a lower limit of 0.3 mr/sec on the indicated value of this quantity. It can be seen that for Technique No. 5, the ΔV differed by 10 to 30 fps for each of the transfers except the 230° abort intercept. This is because some LOS rate over-control still existed when the error was in the plus direction for the 180° intercept, $3\frac{1}{2}$ n.m. and 5 n.m. misses. The ΔV was higher for minus errors on the 210°, 6 n.m. miss case because this tranfer has a LOS rate in the minus direction.

Effect of Range Rate Control - Results of the study indicated that ΔV requirements are not as sensitive to the control of range-rate as to the control of LOS rate. This can be attributed to the fact that the range-rate remains relatively constant during the terminal rendezvous if an intercept course is established and proper control of the LOS rate is maintained. Thus, the main function of a terminal range-rate schedule is to reduce the range-rate at different range intervals to allow an intercept that is compatible with rendezvous. It was also determined, however, that a terminal range-rate schedule for manual control of rendezvous must have both a lower and upper bound on range-rate at each range checkpoint. The reason for this is that the value to which the LOS rate is controlled at each range checkpoint is not a value which will give an exact intercept for every transfer which might be used in a specific mission. Rather, it is a compromised value which gives the best overall results for all possible transfers. Thus, because the LOS rate correction is not one which gives an exact intercept, the range-rate can drop off at any time, depending upon the type of transfer being used, and a miss would occur if a lower limit were not placed on range-rate. Technique No. 1 allowed the range-rate to drop off unchecked for some transfers because no lower limit on range-rate was used. Techniques No. 2 and 3 solved this problem by using the GAEC terminal range-rate schedule. Technique No. 4, again, had the same problem of range-rate dropoff for some transfers because no lower range-rate bound was used. In modifying Technique No. 4 to what has previously been described as Technique No. 5, the problem of range-rate dropoff was solved by using the single range-rate values specified for each range checkpoint as both upper and lower bounds. In other words, the range-rate is controlled to this value regardless of whether the current range-rate is above or below this value at the checkpoint. The range-rate values were chosen so that the range-rate would not be increased at any checkpoint unnecessarily (If parking orbit transfers are used which inherently have much lower terminal range-rates, the range-rate values used in Technique No. 5 would be different). In addition to using the range-rate values in Technique No. 5 as upper and lower bounds, one additional checkpoint was added at 90,000 feet range to control any range-rate dropoff which might occur between the ranges of 20,000 feet and 60,000 feet.

Effect of Combining LOS Rate and Range Rate Corrections - A very significant reduction in ΔV usage resulted when the LOS rate and range-rate corrections were combined into one thrust maneuver at each range checkpoint. Techniques No. 1, 2, and 3 were not designed to use this type of thrusting because the LOS rate and range-rate corrections are usually made at different ranges. This type of thrusting was attempted with the GAEC Technique using the Technique No. 4 nomogram (figure 11). It can readily be seen from table 2 that the ΔV requirements for the Modified GAEC Technique are 20 to 30 fps less than for the unmodified GAEC Technique even though the Modified GAEC Technique runs were made with radar errors. Techniques No. 4 and 5 were specifically designed to take advantage of this type of thrusting in an attempt to approach the efficiency of the PNGS. Except for the aborted runs using certain errors, Technique No. 4 required even less ΔV usage than the Modified GAEC Technique. As indicated above, Technique No. 5 solved the abort problems associated with Technique No. 4. This technique also used less fuel than the Modified GAEC Technique except for the $3\frac{1}{2}$ n.m. miss case with radar LOS errors in the plus direction. As previously pointed out, some overcontrol of the LOS rate occurred using Technique No. 5 when the radar errors had the same sign direction as the LOS rate, i.e., a positive rate with an error in the plus direction or a negative rate with an error in the minus direction.

OPERATIONAL ASPECTS OF MANUAL CONTROL TECHNIQUES

The simulation provided an opportunity to assess the operational implications of the manual control techniques for use in the Lunar Excursion Module (LEM) mission. Specifically, the following points are of interest:

1. The simulation did not use operationally available information on initial conditions such as might be available from the MSFN or out the window of the LEM. It would be expected that the type of trajectory and possibly an estimate of the miss distance after the initiation of rendezvous might be available to the crew from MSFN. Also, LEM attitudes relative to the local horizon could be used by the crew to obtain a clearer mental picture of the LEM's position in the trajectory. This information would help the crew in monitoring the rendezvous and could improve the effectiveness of manual methods.

2. The vector sum method represents a significant ΔV savings and will probably be a mandatory procedure to insure successful rendezvous by manual methods with a critical propellant situation. The method is simple and required relatively little computation by the crew. A similar concept is in use in Gemini where the command pilot resolves the three components of a desired velocity vector correction or command using his incremental velocity indicators (IVI's). However, in the Gemini, the spacecraft computer and platform are required.

3. The two-jet couple was found to be preferable in operation to the four-jet couple for vector sum corrections. The computed vector sum is based on information several seconds old. It is feasible for the pilot to adjust the angle of his correction during the thrusting period to drive both LOS rate and range rate to the desired values simultaneously provided the thrust level is low enough for the pilot to have time to judge rates of change. As a result, changes in LOS rate and range rate can be compensated. The four-jet couple provided too much thrust in some cases to permit the pilot to judge the necessary rate changes. The two-jet couple was found to be satisfactory for all corrections.

4. The use of a manual control technique with range/range-rate checkpoints compatible with the automatic PNGS checkpoints has the effect of greatly simplifying crew procedures during rendezvous. If the PNGS is operating and in use, the crew monitors the PNGS progress at each point and has readily available information as to what range/range-rate relationship should hold. Should the PNGS fail during terminal rendezvous, the crew is provided with an immediate cue at a given checkpoint and a procedure for takeover at that point. The crew then completes the rendezvous by manual procedures. If the PNGS is inoperative, the crew has an effective means of manual rendezvous using the developed technique.

The major significance of this simulation program and its results lies in two areas--first, the ΔV savings through the vector sum method provide a major improvement in manual technique effectiveness and second, the concept of the PNGS and manual range-range-rate schedules being compatible for operation provides a highly significant simplification in crew procedures

CONCLUSIONS

The conclusions obtained from this study are as follows:

1. The ΔV requirements for any manual rendezvous-control technique are much more sensitive to LOS rate control than to range-rate control.

2. Thrusting along the vector sum of the desired range-rate and LOS-rate corrections significantly lowers the ΔV requirements of any rendezvous manual control technique. This type of thrusting is easily executed with the aid of a nomogram to determine the desired direction and scaled azimuth and elevation angle indicators.

3. A single range-rate value can be used at each range checkpoint of the terminal schedule without increasing the ΔV requirements for the maneuver provided the range-rate values are used as both upper and lower bounds. Single range-rate values at each range checkpoint will contribute

to ease of monitoring PNGS operation during this mission phase and will also allow a smooth transition from primary to backup mode of operation in the event of PNGS failure. However, the compatibility of the primary mode with the backup mode also requires that the terminal range-rate schedule for the primary mode be very nearly the same as that for the backup mode.

4. Controlling the LOS-rate to an indicated 0.3 mr/sec causes an overcontrol of the LOS rate when the radar LOS rate errors are the same sign as the actual LOS rate. This, in turn, causes a ΔV penalty from 10 to 20 fps. Based on present radar error estimates, it appears that the best lower limit on LOS rate lies somewhere between 0.3 mr/sec as used in Technique No. 5 and 0.4 mr/sec as used in the GAEC Technique.

RECOMMENDATIONS

Based on the results of this simulation study, it is recommended:

1. That the terminal range-rate schedule shown below be used for the manual backup technique for control of the terminal phase of the LEM/CSM lunar orbit rendezvous and that the range-rate and LOS-rate corrections be made concurrently using a nomogram to determine the desired thrust vector angle with respect to the line of sight. If a parking orbit transfer is used instead of the direct ascent transfer, the first three range checkpoints should be omitted from the schedule because the terminal range-rate is significantly lower for this type of transfer.

Range (feet)	Range-Rate (fps)	LOS-Rate (mr/sec)
120,000	130 *	0.3 - 0.4 **
90,000	100 *	0.3 - 0.4 **
60,000	80 *	0.3 - 0.4 **
30,000	60 *	0.3 - 0.4 **
15,000	40 *	0.3 - 0.4 **
5,000	15 *	0.3 - 0.4 **

*Range-rate values are used as both upper and lower bounds at each checkpoint.

**The optimum value to which the LOS-rate should be controlled at each range checkpoint lies between the values shown. This optimum value should be determined through a digital computer study of this technique and should be based on best available radar information.

2. That the azimuth and elevation angle indicators on the FDAI be designed so that angles can be determined to within three degrees over a range of plus and minus 50 degrees.

3. That the terminal range-rate schedule for the PNGS be as follows (a recent digital computer study of PNGS operation using different terminal range-rate schedules has shown that the schedule given below does not significantly increase the ΔV usage of the primary system):

Range (feet)	Range-Rate (fps)
120,000	100
30,000	60
5,000	15

APPENDIX A

ΔV computation:

$$\Delta V = \int \frac{|T_x| + |T_y| + |T_z|}{m_t} \, dt$$

RCS Fuel:

System "A"

$$W_A = \int \frac{|T_2| + |T_4| + |T_5| + |T_8| + |T_{10}| + |T_{11}| + |T_{13}| + |T_{15}|}{I_{sp(RCS)}} \, dt$$

System "B"

$$W_B = \int \frac{|T_1| + |T_3| + |T_6| + |T_7| + |T_9| + |T_{12}| + |T_{14}| + |T_{16}|}{I_{sp(RCS)}} \, dt$$

APPENDIX B

EULER ANGLE TRANSFORMATION MATRIX

(θ, ψ, ϕ Rotation)

$$\begin{bmatrix} X_B \\ Y_B \\ Z_B \end{bmatrix} \qquad \begin{bmatrix} B \end{bmatrix} \begin{bmatrix} X_I \\ Y_I \\ Z_I \end{bmatrix}$$

where $$\begin{bmatrix} B \end{bmatrix} \qquad \begin{bmatrix} \ell_{11} & \ell_{12} & \ell_{13} \\ \ell_{21} & \ell_{22} & \ell_{23} \\ \ell_{31} & \ell_{32} & \ell_{33} \end{bmatrix}$$

$$\begin{bmatrix} F_X \\ F_Y \\ F_Z \end{bmatrix} \qquad \begin{bmatrix} B \end{bmatrix}^{-1} \begin{bmatrix} T_X \\ T_Y \\ T_Z \end{bmatrix}$$

where $$\begin{bmatrix} B \end{bmatrix}^{-1} = \begin{bmatrix} \ell_{11} & \ell_{21} & \ell_{31} \\ \ell_{12} & \ell_{22} & \ell_{32} \\ \ell_{13} & \ell_{23} & \ell_{33} \end{bmatrix}$$

$$\ell_{11} = \cos\psi \cos\theta$$

$$\ell_{12} = \sin\psi$$

$$\ell_{13} = -\cos\psi \sin\theta$$

$$\ell_{21} = \sin\phi \sin\theta - \cos\phi \sin\psi \cos\theta$$

$$\ell_{22} = \cos\phi \cos\psi$$

$$\ell_{23} = \sin\phi \cos\theta + \cos\phi \sin\psi \sin\theta$$

$$\ell_{31} = \cos\phi \sin\theta + \sin\phi \sin\psi \cos\theta$$

$$\ell_{32} = -\sin\phi \cos\psi$$

$$\ell_{33} = \cos\phi \cos\theta - \sin\phi \sin\psi \sin\theta$$

$$\begin{bmatrix} \dot{\theta} \\ \dot{\psi} \\ \dot{\phi} \end{bmatrix} = \begin{bmatrix} \dfrac{\cos \phi}{\cos \psi} & \dfrac{\sin \phi}{\cos \psi} & 0 \\ \sin \phi & \cos \phi & 0 \\ \tan \psi \cos \phi & -\tan \psi \sin \phi & 1 \end{bmatrix} \begin{bmatrix} q \\ r \\ p \end{bmatrix}$$

$$\begin{bmatrix} \epsilon_{\theta B} \\ \epsilon_{\psi B} \\ \epsilon_{\phi B} \end{bmatrix} = \begin{bmatrix} \cos \psi \cos \phi & \sin \phi & 0 \\ -\cos \psi \sin \phi & \cos \phi & 0 \\ \sin \psi & 0 & 1 \end{bmatrix} \begin{bmatrix} \epsilon_{\theta} \\ \epsilon_{\psi} \\ \epsilon_{\phi} \end{bmatrix}$$

APPENDIX C

GAEC Technique

The tasks given below are followed in numerical order at each range checkpoint:

1. Null azimuth and elevation angles with pitch and yaw maneuvers of spacecraft;

2. Roll spacecraft to null either azimuth rate or elevation rate depending upon which is less (i.e., null smallest rate);

3. Thrust with translation jets perpendicular to LOS to control remaining LOS rate to an indicated plus (or minus) 0.4 mr/sec;

4. Thrust with translation jets along LOS to control range-rate within the boundaries given in the schedule below.

Range-Range Rate Schedule

Range Checkpoint (feet)	Range-Rate (fps)
121,500	70 - 205
97,000	80 - 175
79,000	90 - 140
61,000	80 - 120
36,500	70 - 95
18,000	55 - 65
4,500	12 - 18

Technique No. 1

The following tasks are performed in numerical order at each range checkpoint:

1. Null azimuth elevation angles with pitch and yaw maneuvers of spacecraft;

2. Control range-rate down to value specified in schedule below by thrusting with translation jets along LOS (if range-rate is below value specified in schedule , let it remain as is);

Range-Range Rate Schedule

Range Checkpoint	Range-Rate
91,000	100
61,000	80
30,500	60
15,000	40
4,500	18

Upon a range-rate drop of 10% between any two range checkpoints, the LOS rate is controlled down to 1.0 mr/sec using the same attitude and translation maneuvers as in the GAEC Technique.

Technique No. 4

The following steps are performed in numerical order at each range checkpoint:

1. Null azimuth and elevation angles with pitch and yaw maneuvers of spacecraft;

2. Roll spacecraft to null azimuth or elevation rate, whichever is less;

3. Determine required range-rate correction ($\Delta\dot{R}$) by subtracting range-rate in schedule given below from displayed range-rate (if displayed range-rate is already below value given in schedule, $\Delta\dot{R} = 0$);

4. Determine required LOS rate correction ($\Delta\omega$) by subtracting LOS rate in schedule below from displayed LOS rate (if displayed LOS rate is already below value given in schedule,   = 0);

5. Compute required LOS-rate correction in feet/second using the equation $\Delta V_{\dot{E}} = (R)(\Delta\dot{E} \times 10^{-3})$ fps (R and $\dot{E}$ are in units of feet and milliradians/second respectively);

6. Obtain required azimuth or elevation angle from nomogram in figure 11.

7. Control attitude of spacecraft to the required azimuth or elevation angle and maintain the remaining LOS angle at zero;

8. Thrust in the required direction until the LOS angular rate and range-rate have been reduced to the desired values for these parameters corresponding to the current range checkpoint.

Range, Range-Rate and LOS Rate Schedule

Range Checkpoint (feet)	Range-Rate fps	LOS Rate mr/sec
120,000	100	0.25
60,000	80	0.25
30,000	60	0.20
15,000	40	0.20
4,500	18	0.20

Technique No. 5

The following steps are performed in numerical order at each range checkpoint:

1. Null azimuth and elevation angles with pitch and yaw maneuvers of spacecraft;

2. Roll spacecraft to null azimuth or elevation rate, whichever is less;

3. Determine current LOS-rate and range-rate from instrument displays and locate intersection of these two values on nomogram for current range checkpoint. This intersection determines the correct LOS angle to be used for the upcoming thrust maneuver (An intersection above the 45^o line indicates that the vertical jets should be used if the LOS rate to be controlled lies in the spacecraft elevation plane or that the horizontal jets should be used if the LOS rate to be controlled lies in the azimuth plane. This allows the LOS angle to be maintained below 45^o.);

4. Control the attitude of the spacecraft to the required azimuth or elevation angle;

5. Thrust in the required direction until the LOS-rate and range-rate have been reduced to the lowest value given on the scales for the current range checkpoint.

APPENDIX D

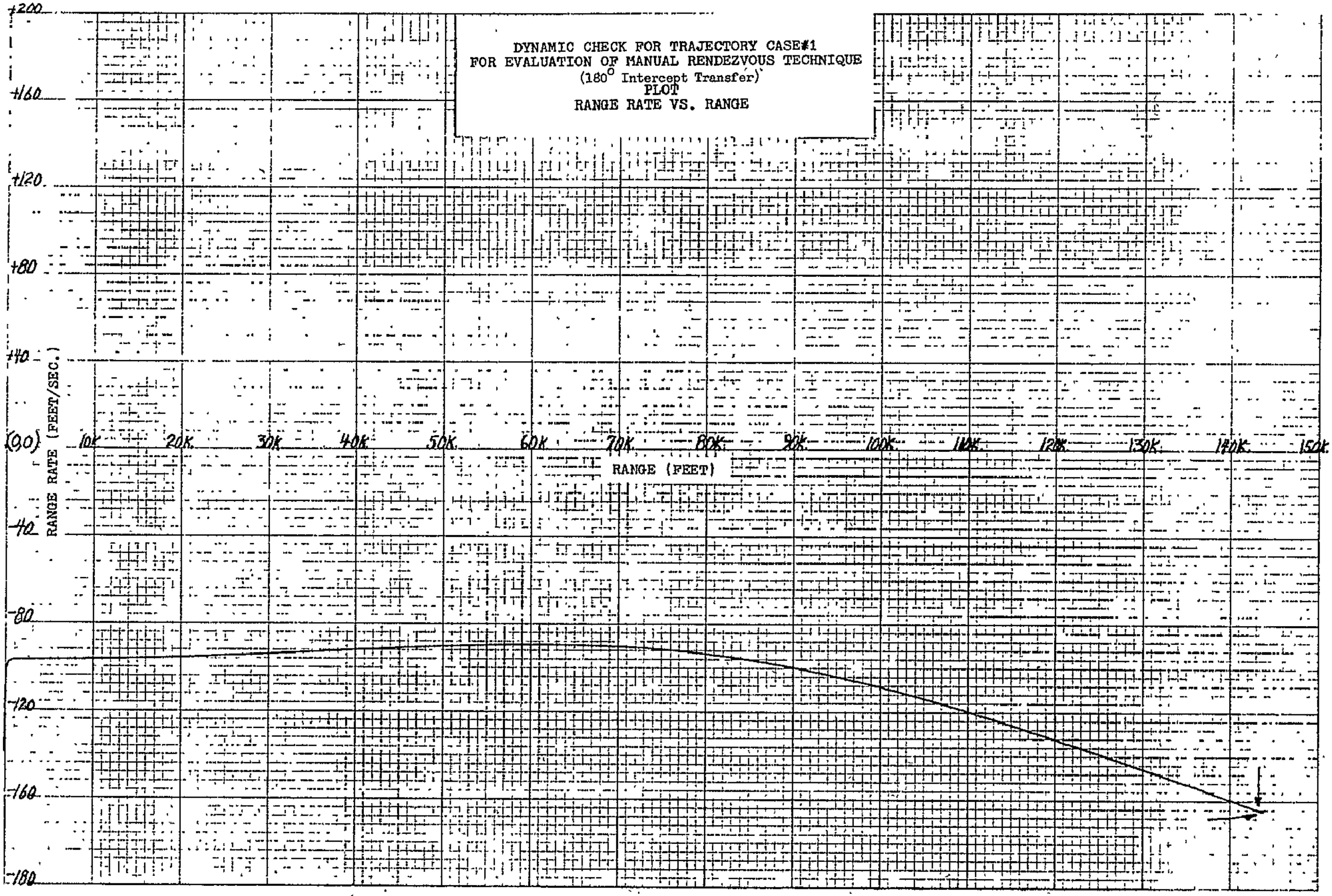
DYNAMIC CHECK FOR TRAJECTORY CASE#1
FOR EVALUATION OF MANUAL RENDEZVOUS TECHNIQUE
(180° Intercept Transfer)
PLOT
RANGE RATE VS. RANGE
RANGE RATE (FEET/SEC.)
RANGE (FEET)
+200
+160
+120
+80
+40
(0,0)
-40
-80
-120
-160
-180
10K
20K
30K
40K
50K
60K
70K
80K
90K
100K
110K
120K
130K
140K
150K

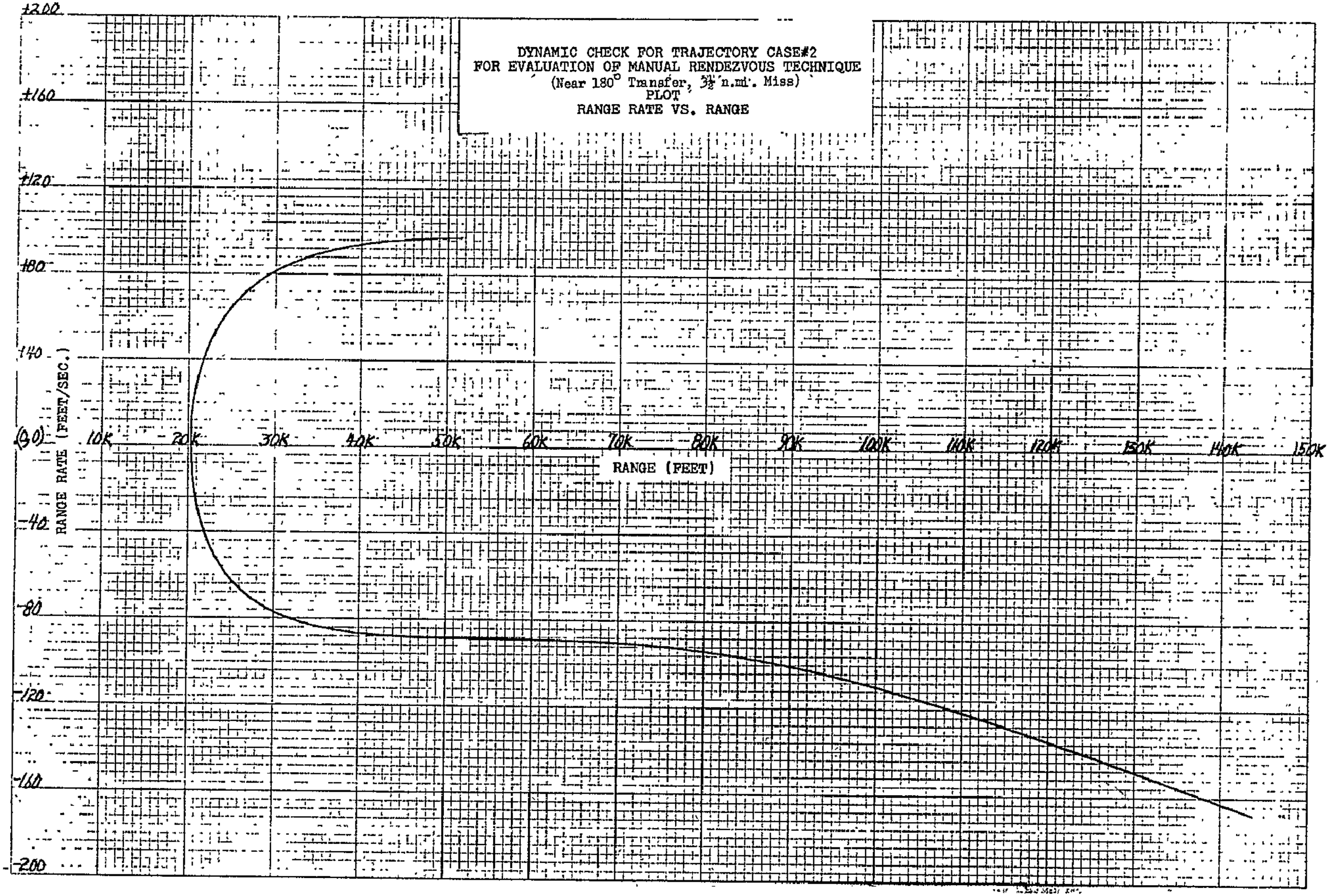
DYNAMIC CHECK FOR TRAJECTORY CASE#2
FOR EVALUATION OF MANUAL RENDEZVOUS TECHNIQUE
(Near 180° Transfer, 3½ n.mi. Miss)
PLOT
RANGE RATE VS. RANGE
RANGE RATE (FEET/SEC.)
RANGE (FEET)
+200
+160
+120
+80
+40
(0)
-40
-80
-120
-160
-200
10K
20K
30K
40K
50K
60K
70K
80K
90K
100K
110K
120K
130K
140K
150K

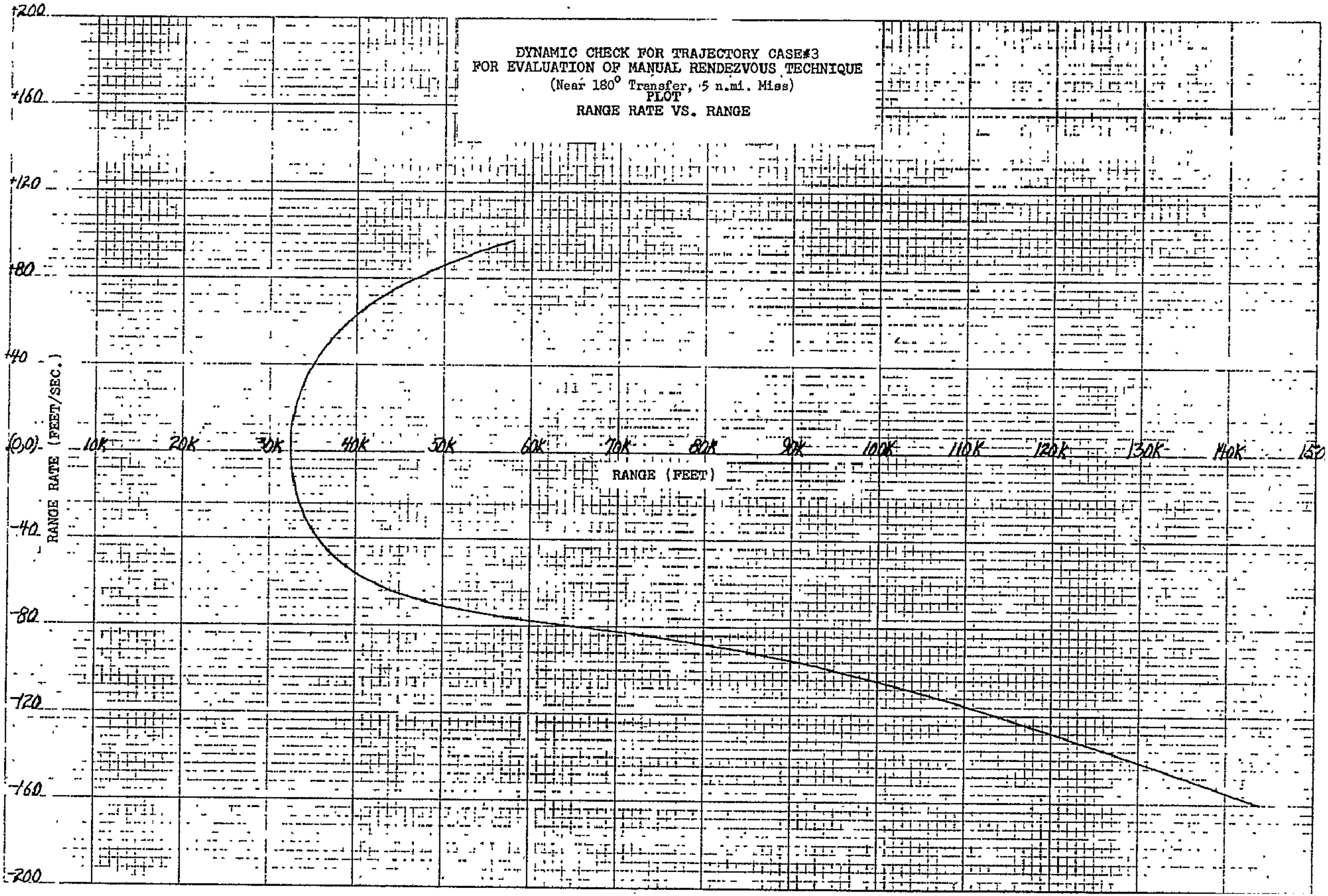
DYNAMIC CHECK FOR TRAJECTORY CASE#3
FOR EVALUATION OF MANUAL RENDEZVOUS TECHNIQUE
(Near 180° Transfer, 5 n.mi. Miss)
PLOT
RANGE RATE VS. RANGE
RANGE RATE (FEET/SEC.)
RANGE (FEET)
+200
+160
+120
+80
+40
(0,0)
-40
-80
-120
-160
-200
10K
20K
30K
40K
50K
60K
70K
80K
90K
100K
110K
120K
130K
140K
150

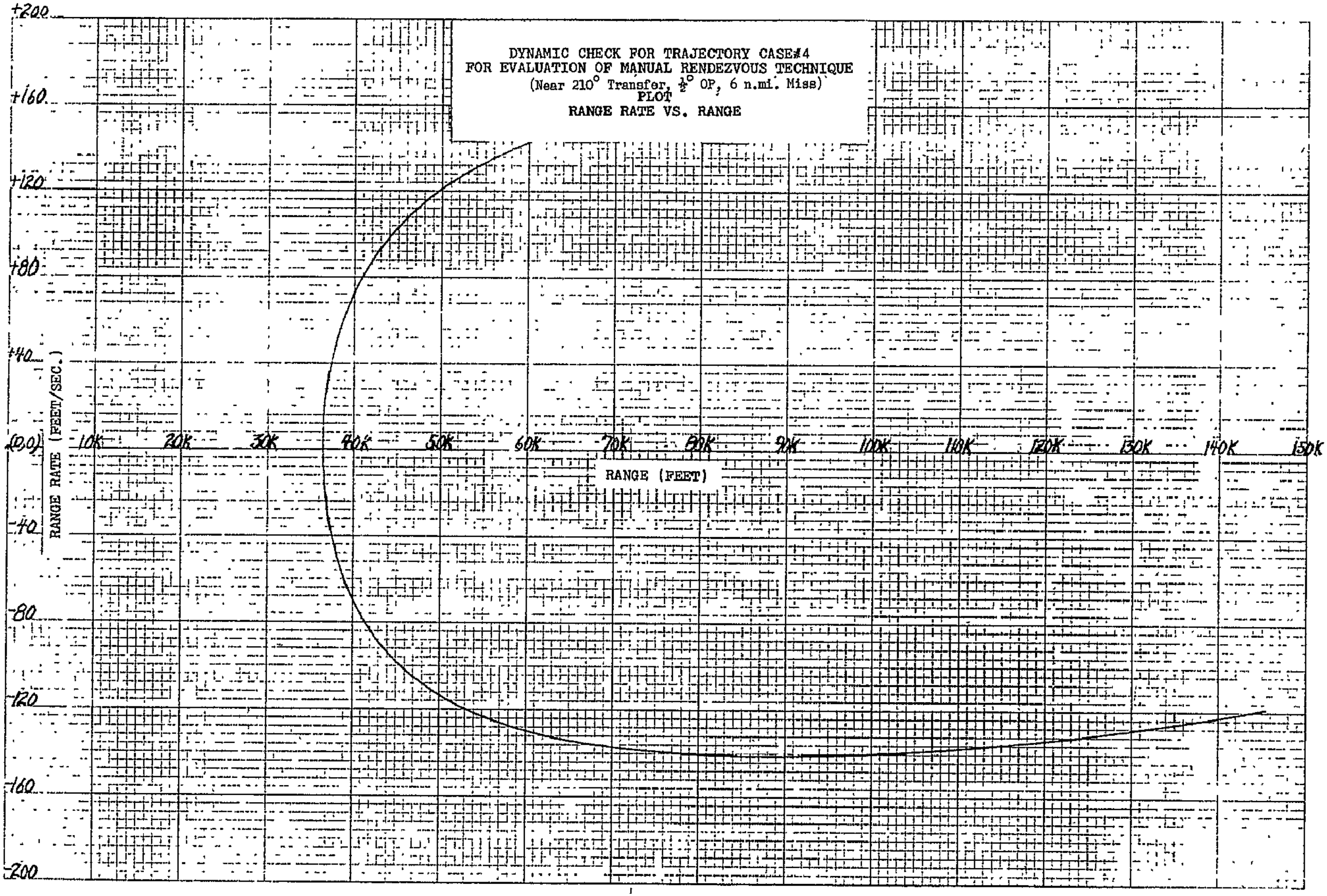
DYNAMIC CHECK FOR TRAJECTORY CASE#4
FOR EVALUATION OF MANUAL RENDEZVOUS TECHNIQUE
(Near 210° Transfer, ½° OP, 6 n.mi. Miss)
PLOT
RANGE RATE VS. RANGE
RANGE RATE (FEET/SEC.)
RANGE (FEET)
+200
+160
+120
+80
+40
(0,0)
-40
-80
-120
-160
-200
10K
20K
30K
40K
50K
60K
70K
80K
90K
100K
110K
120K
130K
140K
150K

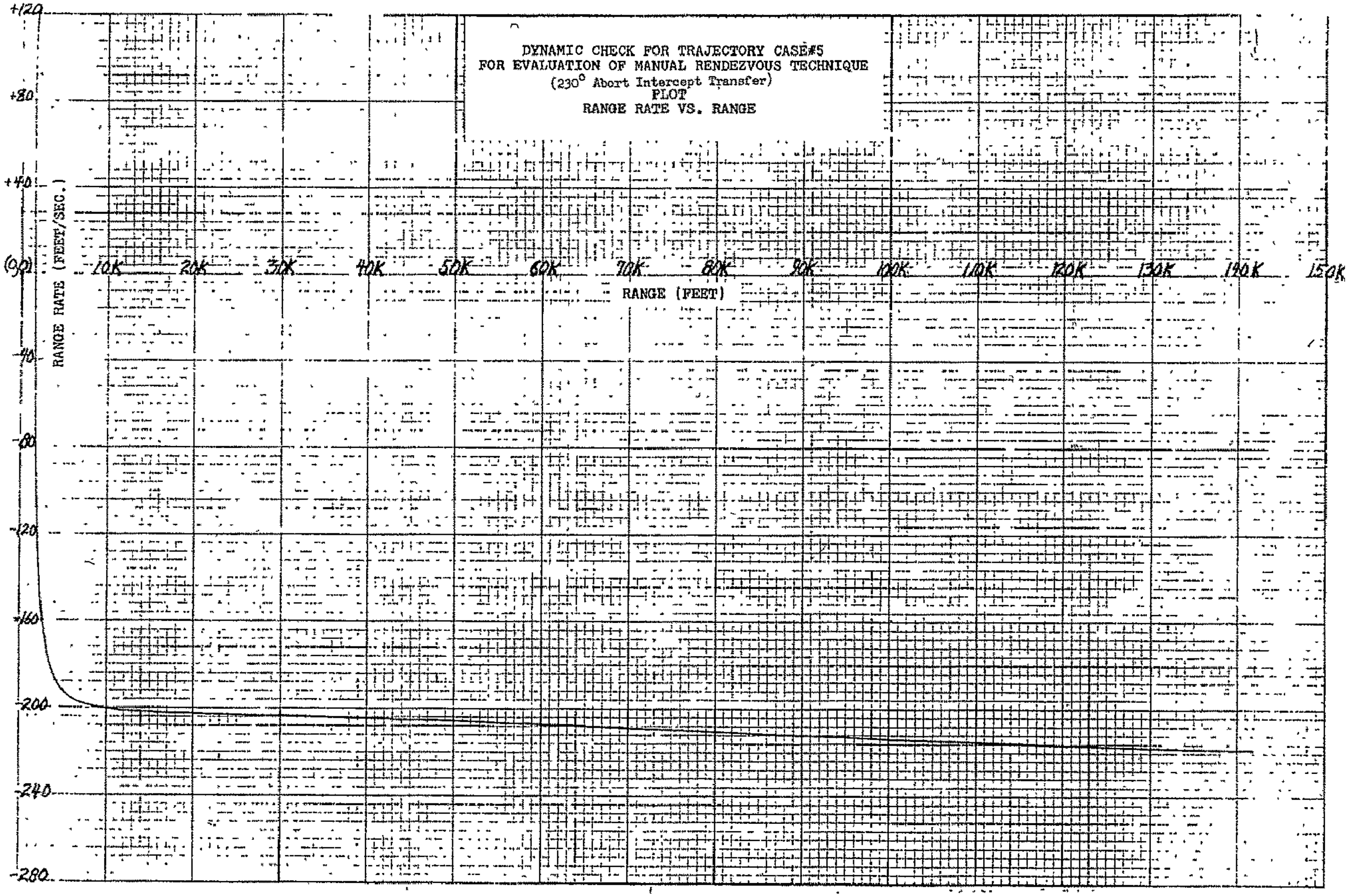
DYNAMIC CHECK FOR TRAJECTORY CASE#5
FOR EVALUATION OF MANUAL RENDEZVOUS TECHNIQUE
(230° Abort Intercept Transfer)
PLOT
RANGE RATE VS. RANGE
RANGE RATE (FEET/SEC.)
RANGE (FEET)
+120
+80
+40
(0,0)
-40
-80
-120
-160
-200
-240
-280
10K
20K
30K
40K
50K
60K
70K
80K
90K
100K
110K
120K
130K
140K
150K

APPENDIX E

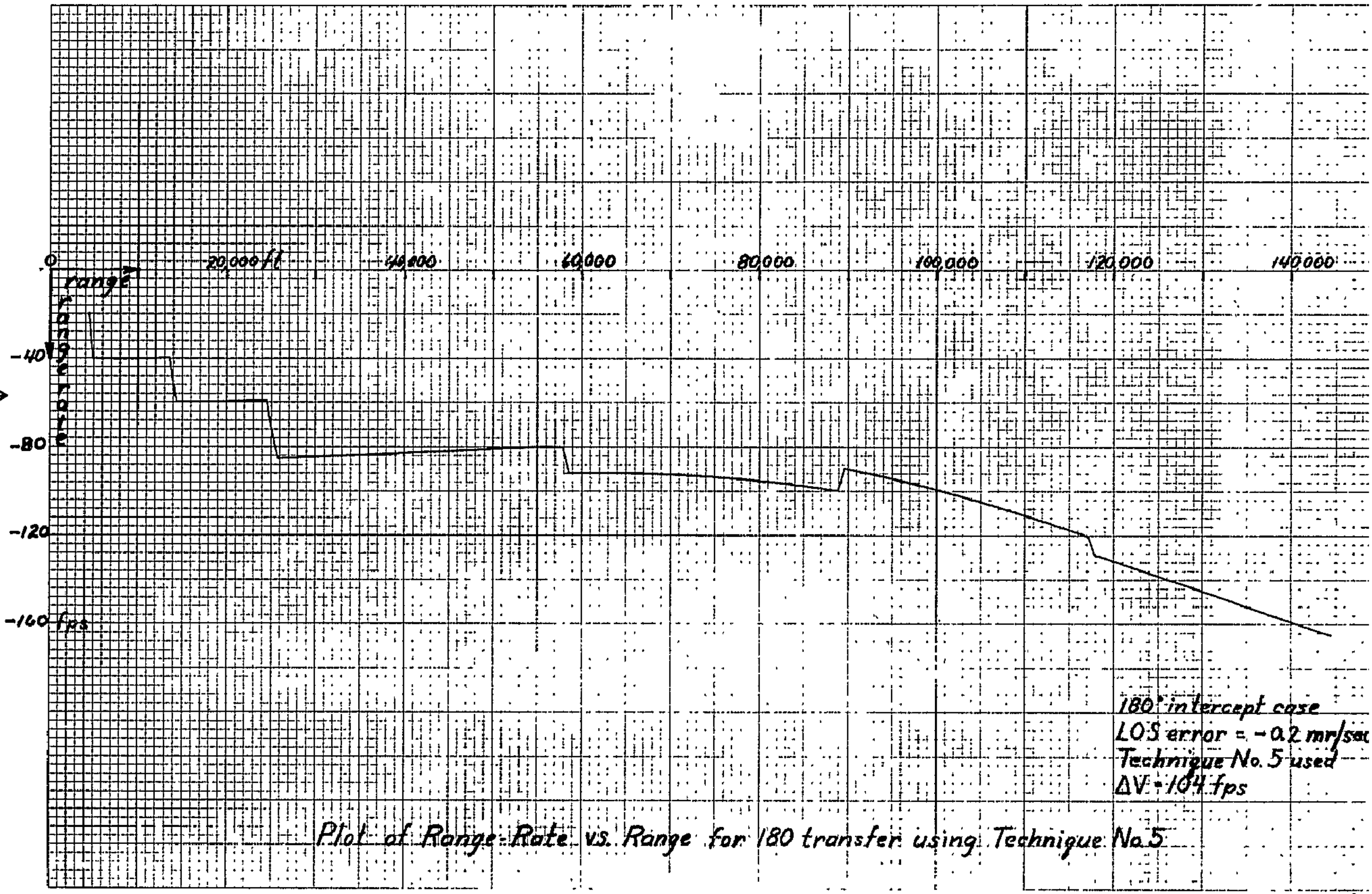

Plot of Range-Rate vs. Range for 180 transfer using Technique No. 5

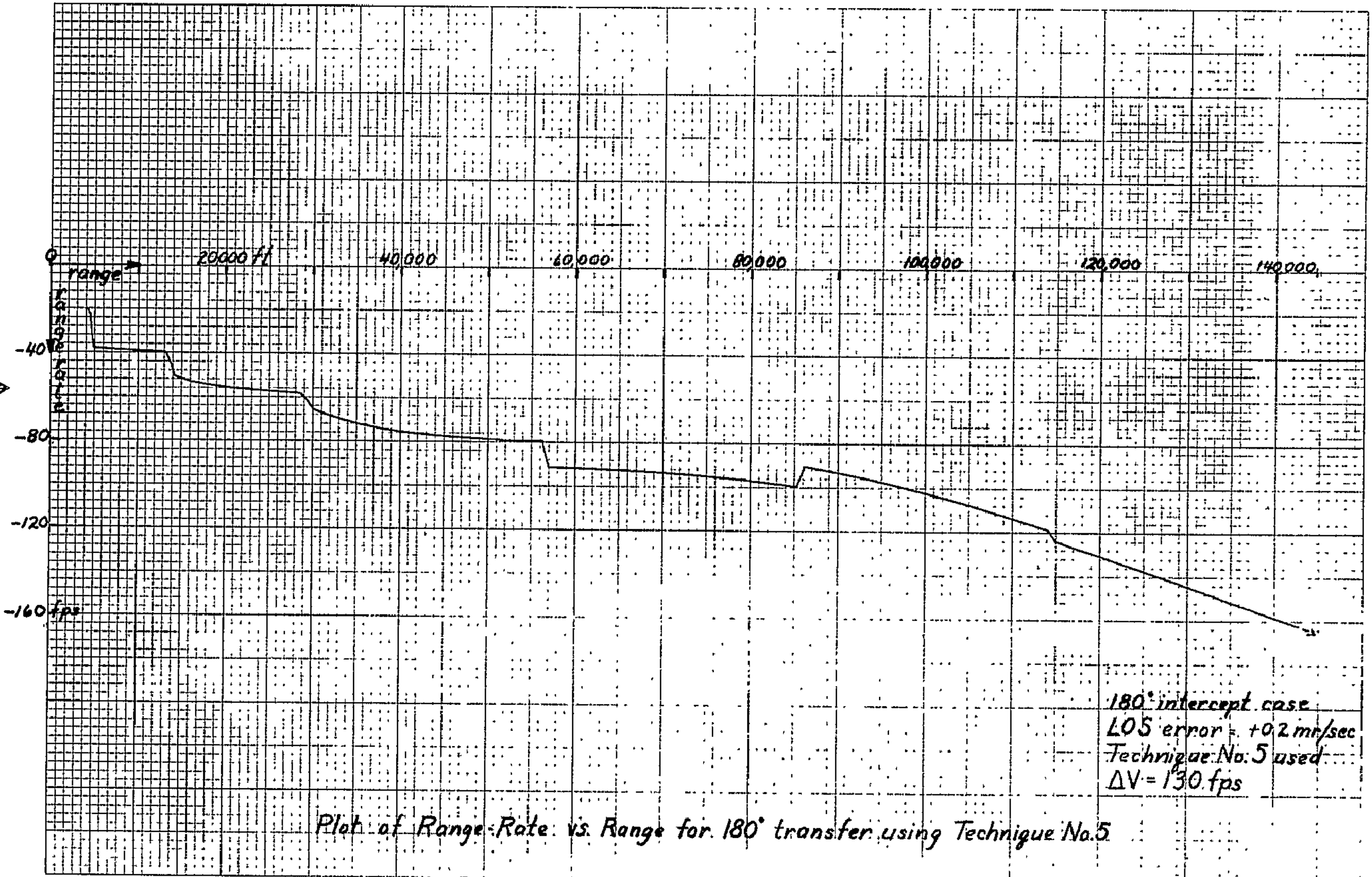

Plot of Range Rate vs. Range for 180° transfer using Technique No.5

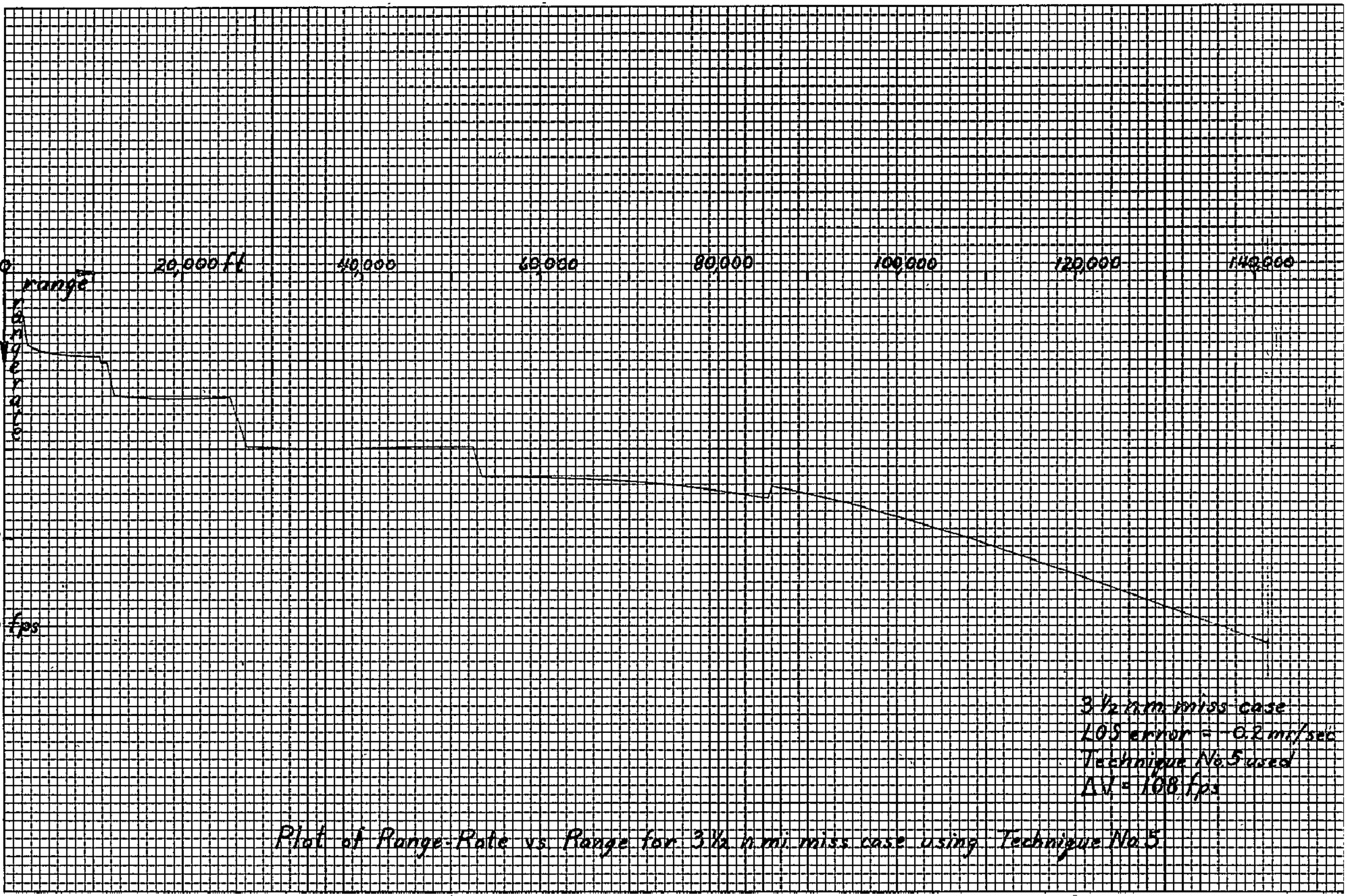

Plot of Range-Rate vs Range for 3½ n.mi. miss case using Technique No.5

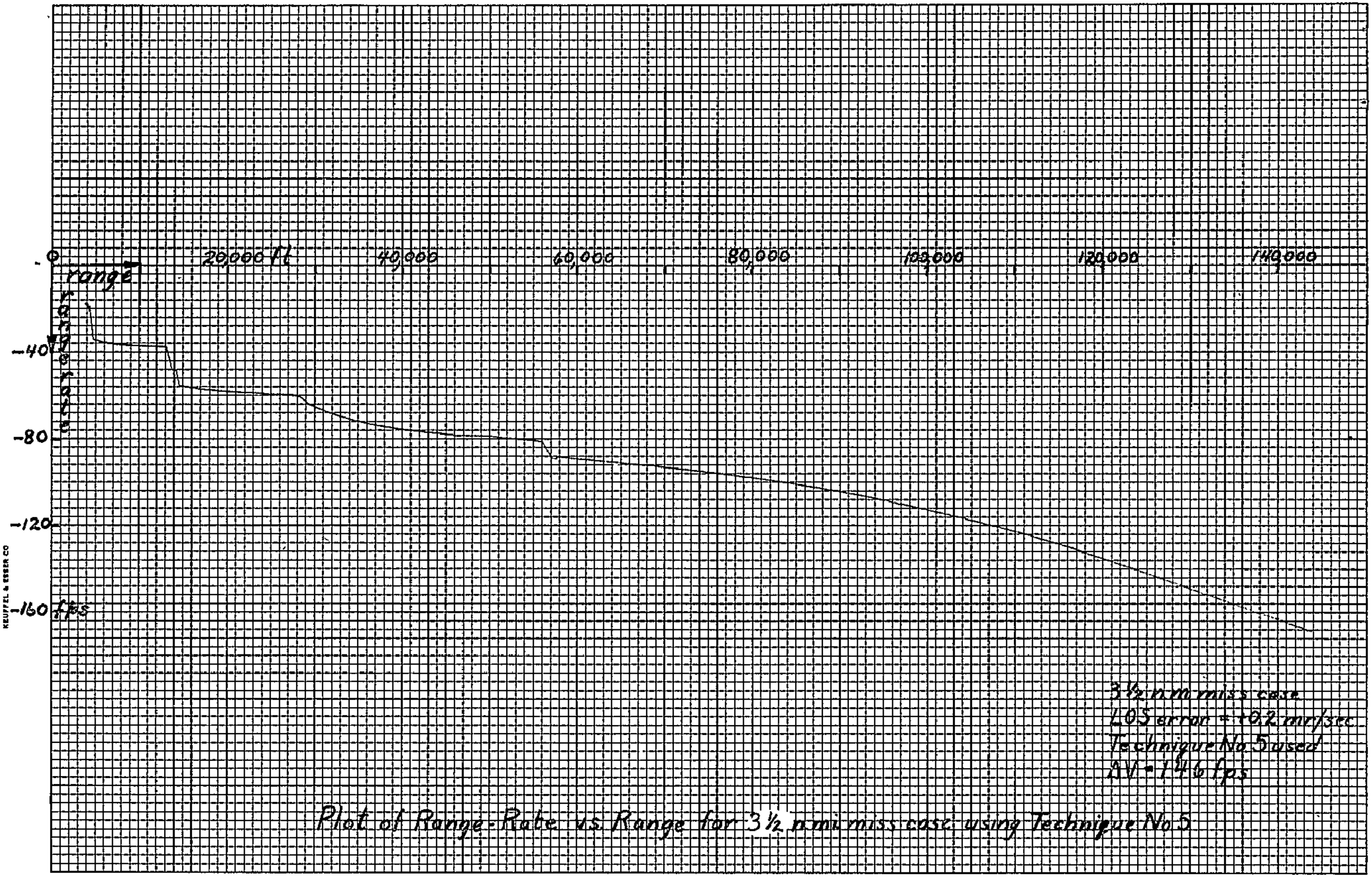

Plot of Range-Rate vs Range for 3½ n.mi. miss case using Technique No 5

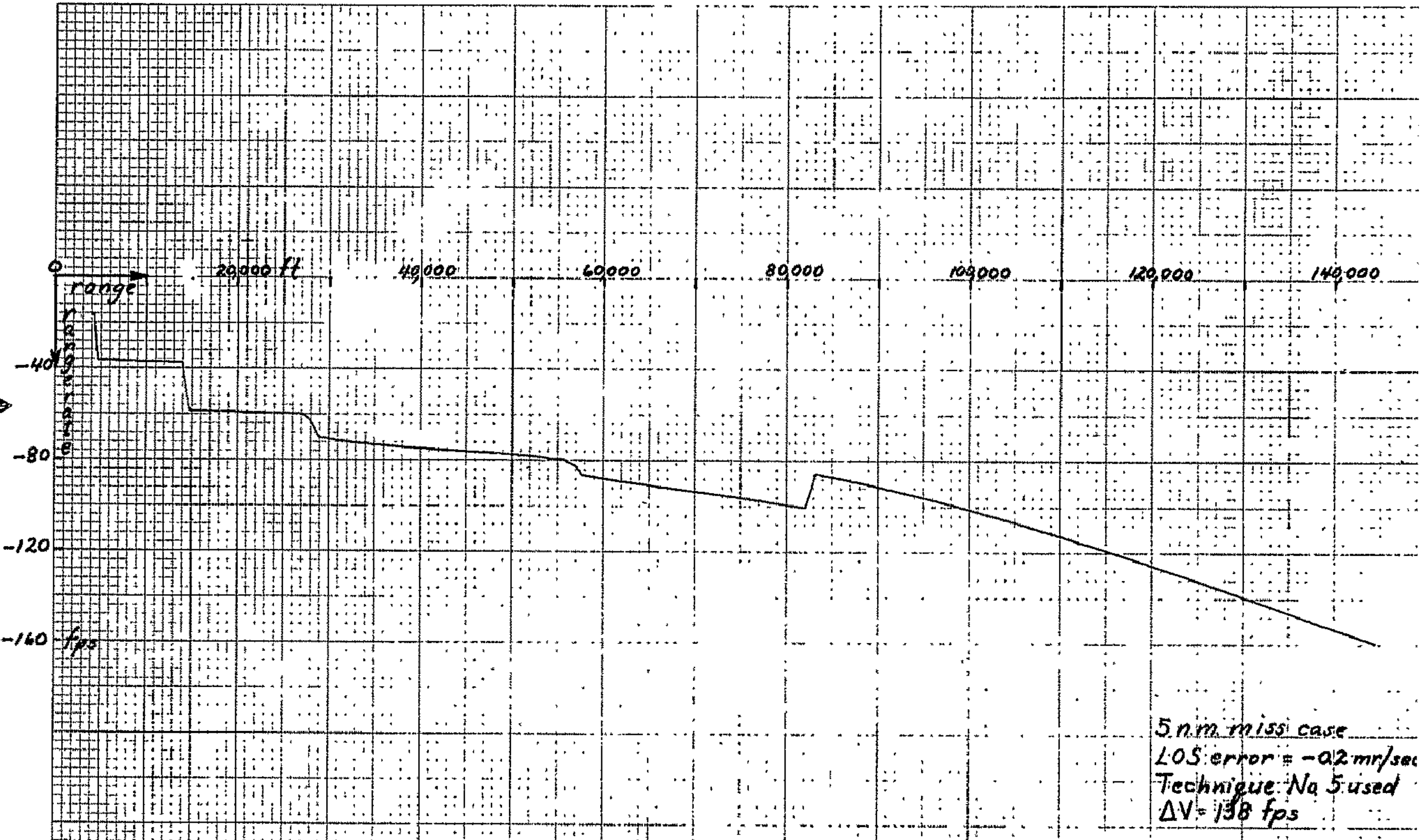

Plot of Range-Rate vs Range for 5 n.m. miss case using Technique No. 5

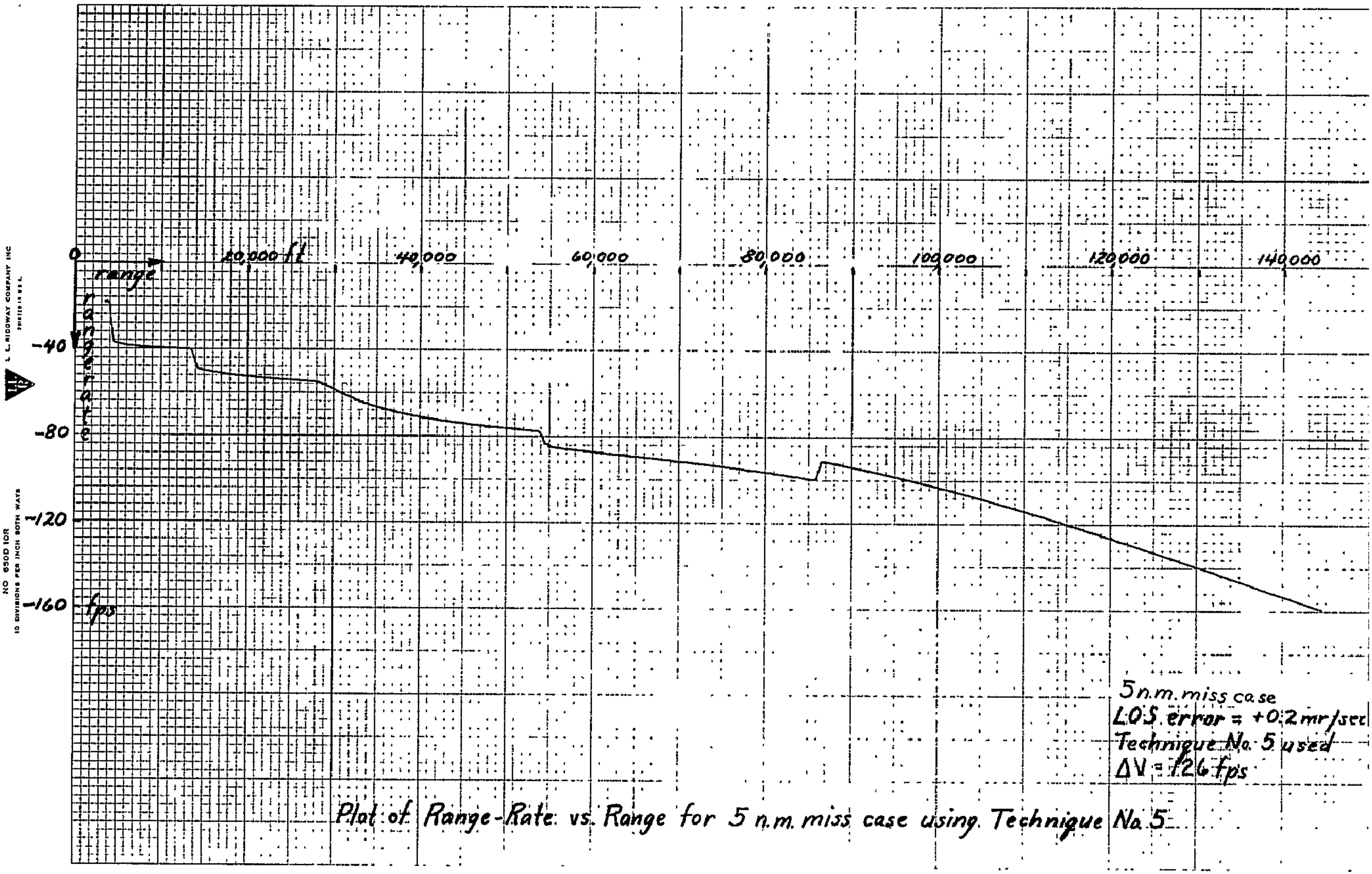

Plot of Range-Rate vs. Range for 5 n.m. miss case using Technique No. 5

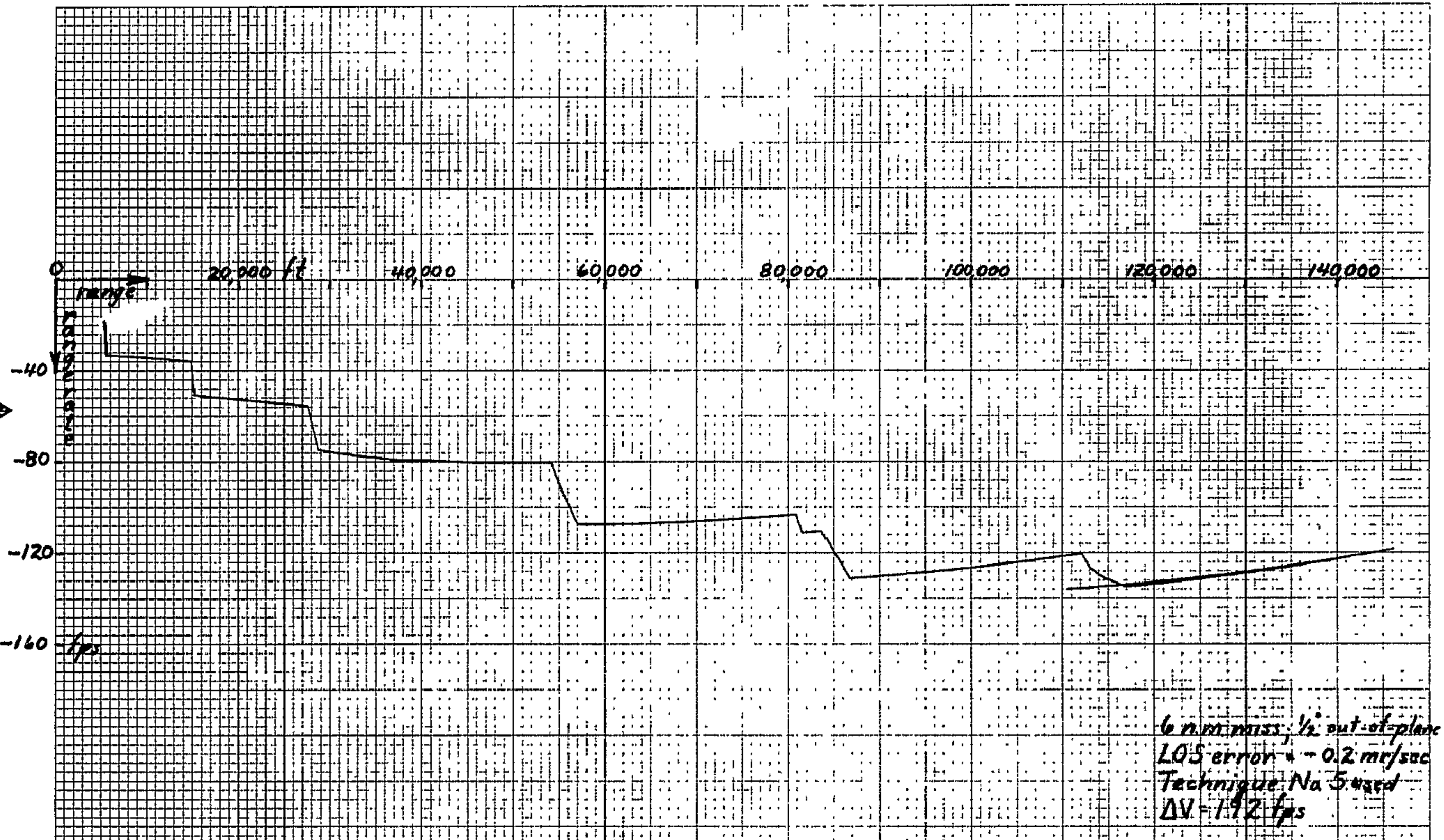

Plot of Range-Rate vs. Range for 6 n.m. miss case using Technique No. 5

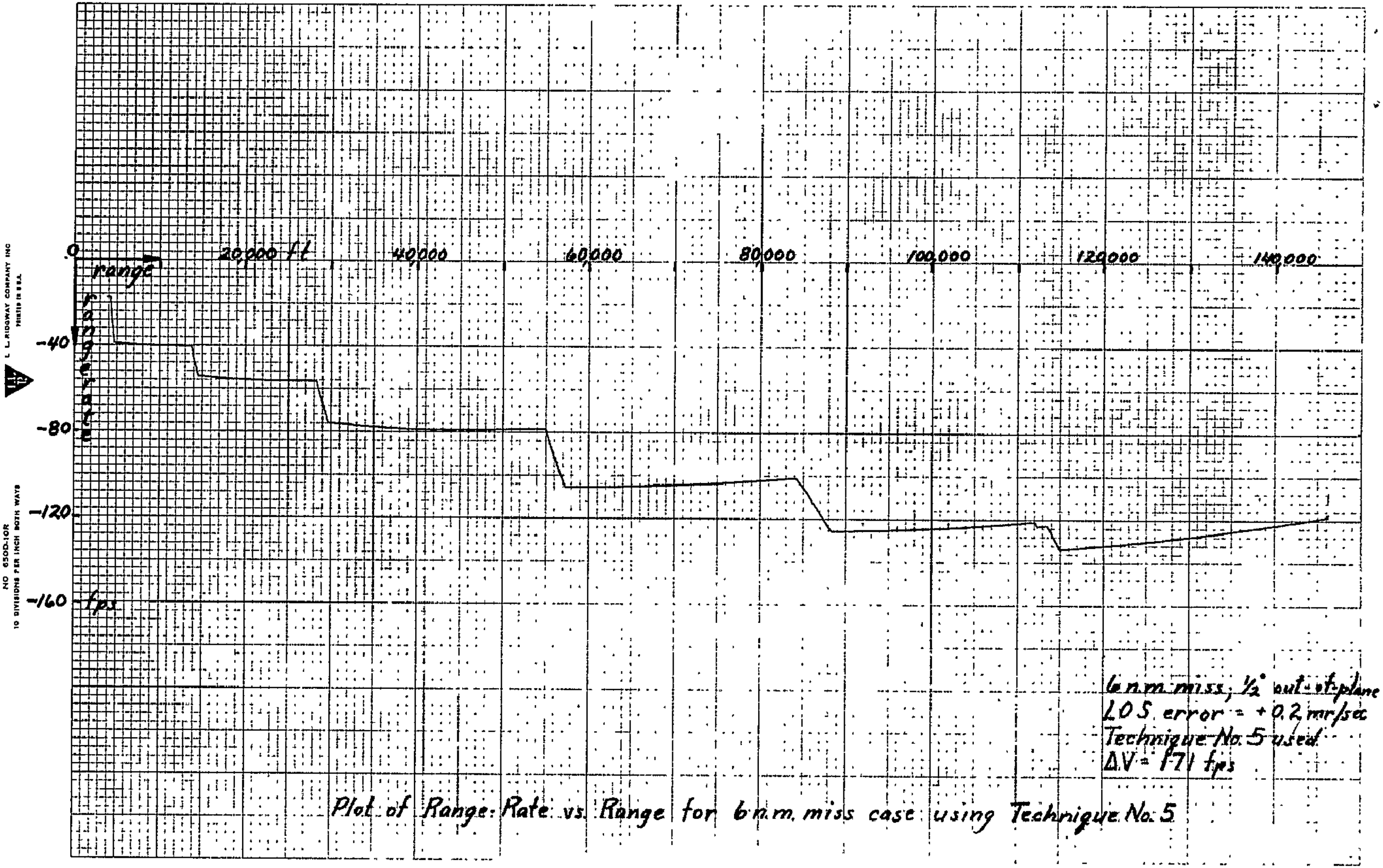

Plot of Range-Rate vs. Range for 6 n.m. miss case using Technique No. 5

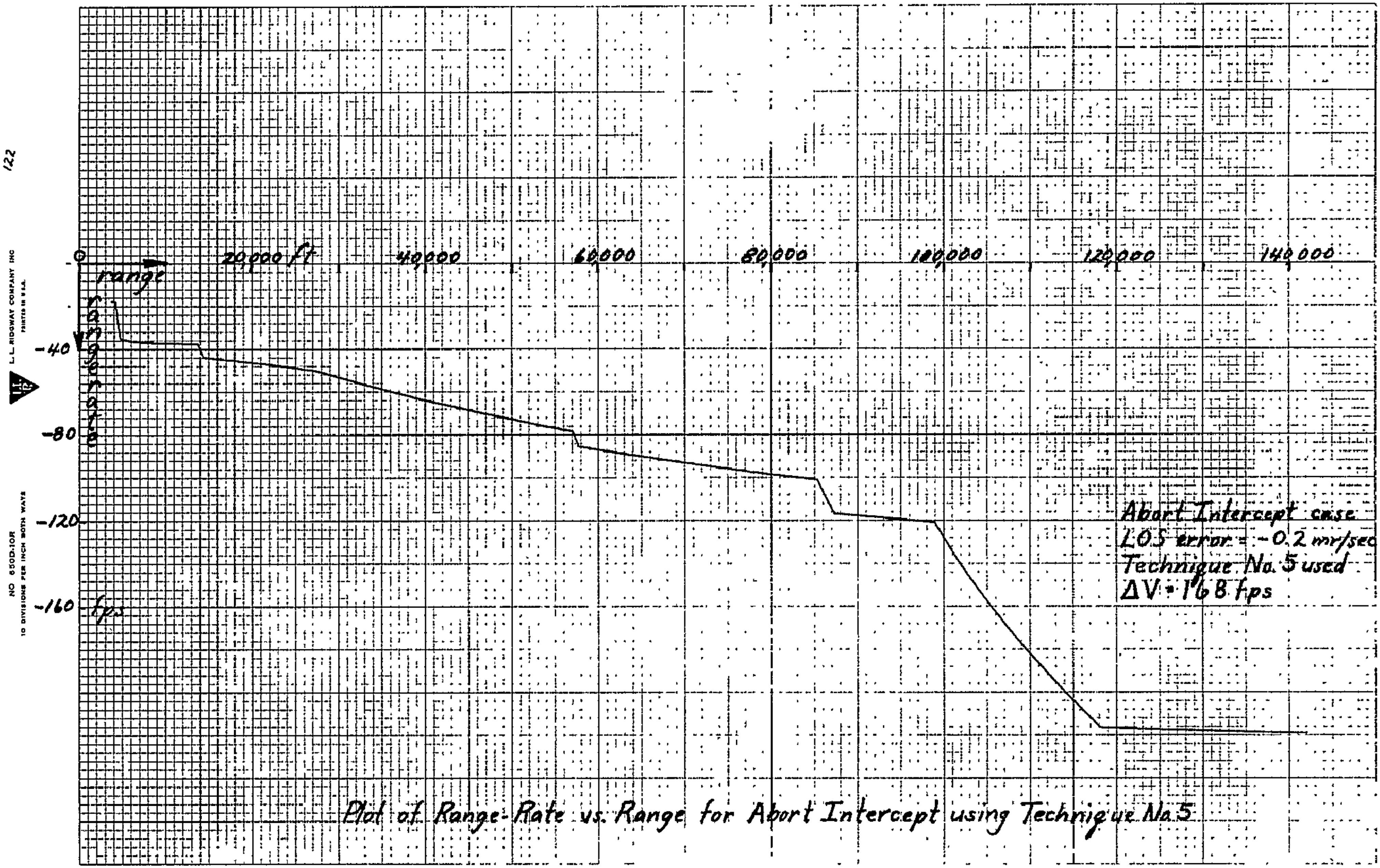

Plot of Range-Rate vs. Range for Abort Intercept using Technique No. 5

TEST CASE	PROBLEM VARIABLES						
	λ DEG.	X FEET	Y FEET	Z FEET	$\dot{X}$ FEET/ SEC.	$\dot{Y}$ FEET/ SEC.	$\dot{Z}$ FEET/ SEC.
#1 HCHMANN INTERCEPT	111.75	-139237	0	-38555	146.793	0	86.939
#2 31/2 N. MI. MISS:	111.75	-139237	0	-38555	146.793	5	98.939
#3 5 N. MI. MISS :	111.75	-139237	0	-38555	146.793	5	68.939
#4 6 N. MI. MISS:	160.96	-123166	65535	43502	76.13	-70.95	-76.06
#5 ABORT 365 sec. after start of power descent	196.62	-132748	0	51302	192.07	0	-110.035
INITIAL MASS: 159SLUGS for cases 1,2,3,&4.							
INITIAL MASS: 248 SLUGS for case 5.							

Table 1.-Initial Conditions for Test Cases

TECHNIQUE	LOS Rate Errors	TEST CASE RESULTS***				
		180° Intercept	Near 180° $3\frac{1}{2}$ n.mi. miss	Near 180° 5 n.mi. miss	210°, $\frac{1}{2}$° OP 6 n.mi. miss	Abort Intercept
GAEC	None	114	145	165	238	201
	±0.2 mr/sec	—	—	—	259	—
Technique No. 1	None	113	171	174	—	198
	±0.2 mr/sec	—	—	—	—	—
Technique No. 2	None	—	—	—	256	200
	±0.2 mr/sec	—	—	—	—	—
Technique No. 3	None	—	—	—	236	—
	±0.2 mr/sec	—	—	—	253	—
Modified GAEC (VS)*	None	—	—	—	205	—
	±0.2 mr/sec	—	115	146	204	177
Technique No. 4 (VS)*	None	—	—	—	176	—
	±0.2 mr/sec	—	(+)abort (-) 106	(+)abort	(+)179 (-)201	—
Technique No. 5 (VS)*	None	—	—	—	—	—
	±0.2 mr/sec	(+)127 (-)102	(+)148 (-)115	(+)138 (-)126	(+)171 (-)192	169
PNGS**	—	88	99	104	126	146

*(VS) = vector sum technique used
**No PNGS drifts or errors were assumed
***The (+) and (-) in the test case results columns apply to results corresponding to the respective sign of the COS rate error.

Table 2.-Average ΔV usage for each test case in fps

FIGURES

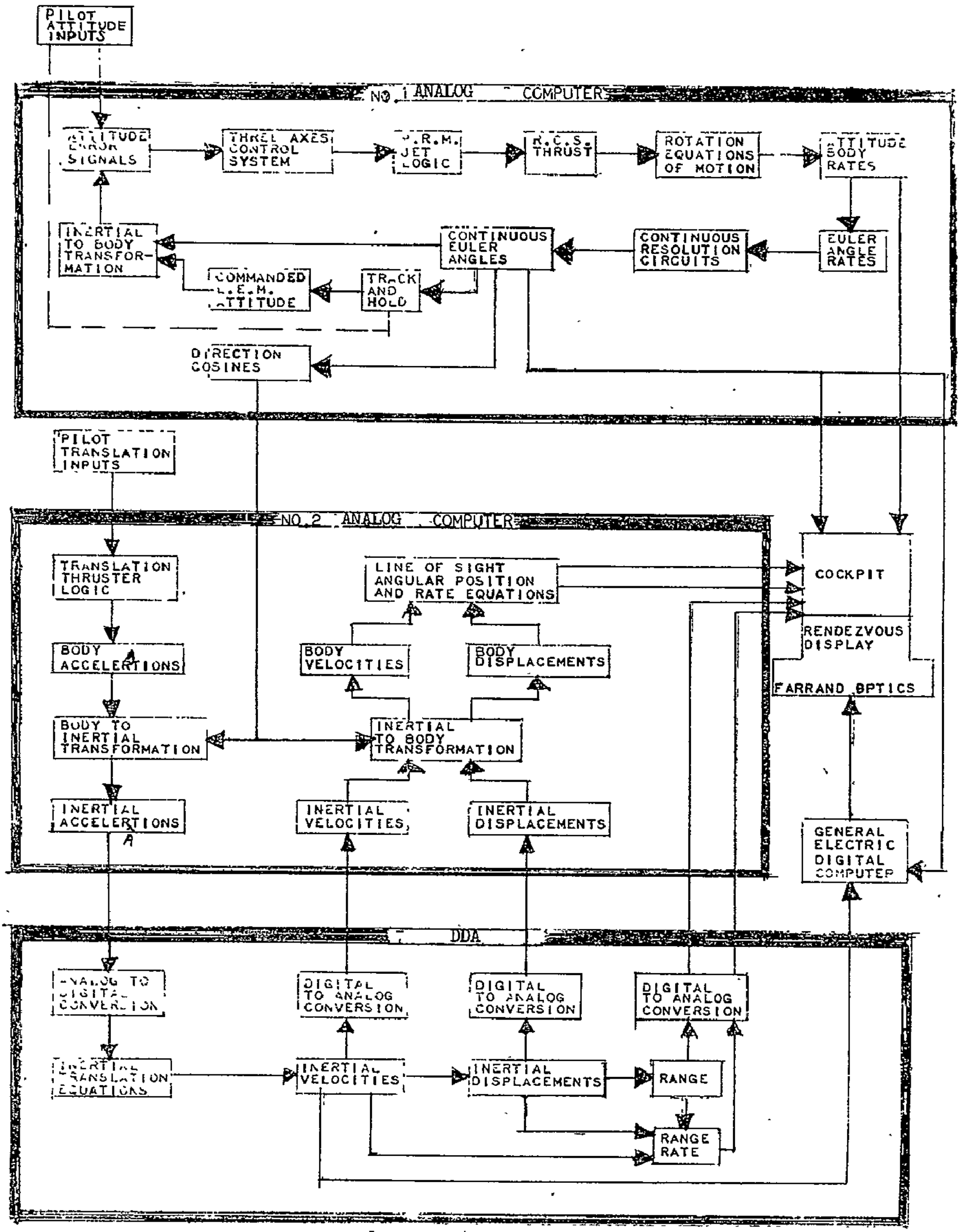
PILOT ATTITUDE INPUTS
NO 1 ANALOG COMPUTER
ATTITUDE ERROR SIGNALS
THREE AXES CONTROL SYSTEM
R.C.S. THRUST
ROTATION EQUATIONS OF MOTION
ATTITUDE BODY RATES
INERTIAL TO BODY TRANSFORMATION
CONTINUOUS EULER ANGLES
CONTINUOUS RESOLUTION CIRCUITS
EULER ANGLE RATES
COMMANDED L.E.M. ATTITUDE
TRACK AND HOLD
DIRECTION COSINES
PILOT TRANSLATION INPUTS
NO 2 ANALOG COMPUTER
TRANSLATION THRUSTER LOGIC
LINE OF SIGHT ANGULAR POSITION AND RATE EQUATIONS
COCKPIT
BODY ACCELERATIONS
BODY VELOCITIES
BODY DISPLACEMENTS
RENDEZVOUS DISPLAY
FARRAND OPTICS
BODY TO INERTIAL TRANSFORMATION
INERTIAL TO BODY TRANSFORMATION
INERTIAL ACCELERATIONS
INERTIAL VELOCITIES
INERTIAL DISPLACEMENTS
GENERAL ELECTRIC DIGITAL COMPUTER
DDA
ANALOG TO DIGITAL CONVERSION
DIGITAL TO ANALOG CONVERSION
DIGITAL TO ANALOG CONVERSION
DIGITAL TO ANALOG CONVERSION
INERTIAL TRANSLATION EQUATIONS
INERTIAL VELOCITIES
INERTIAL DISPLACEMENTS
RANGE
RANGE RATE

Figure 1

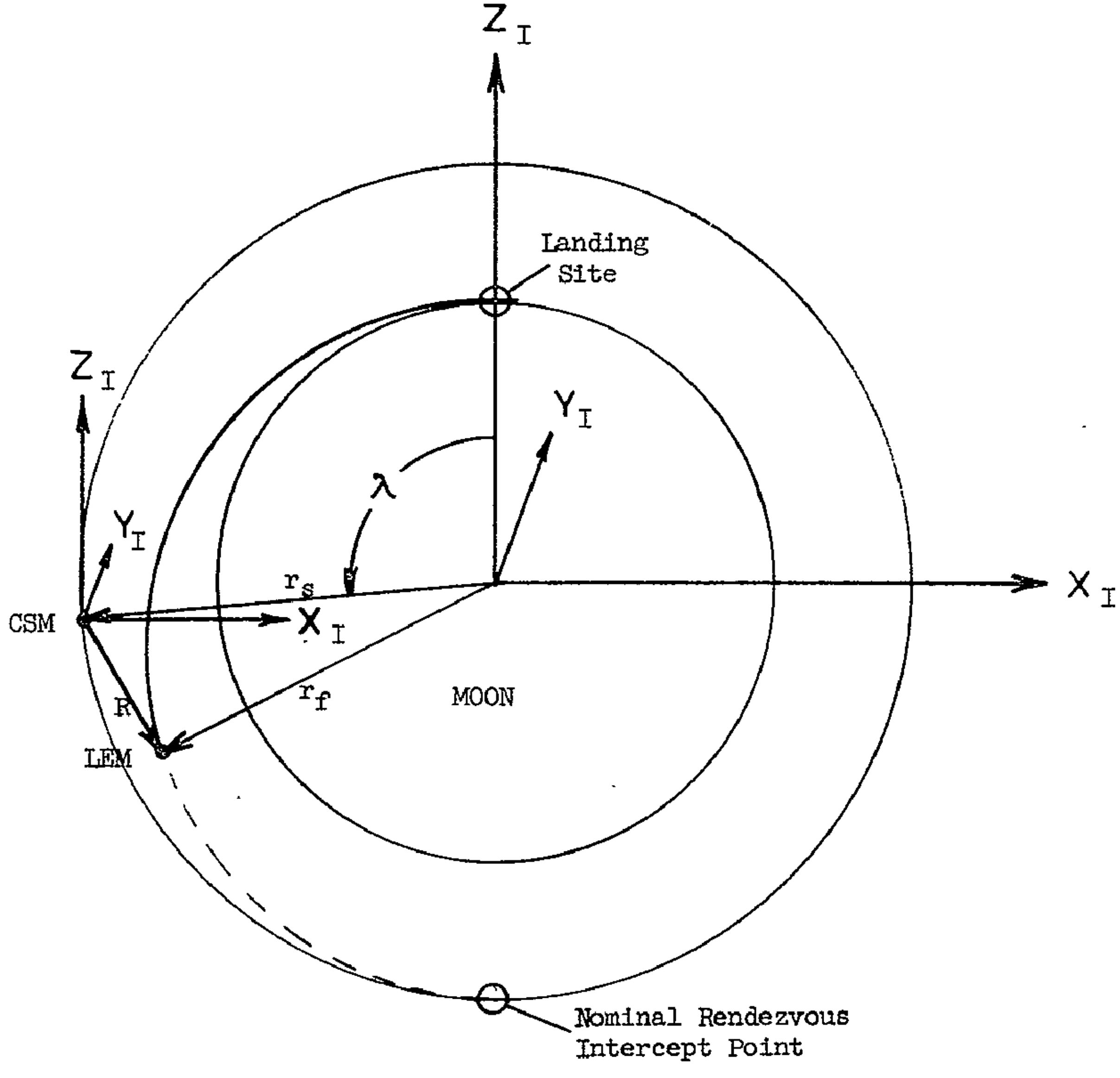

Figure 2 - Inertial Reference Frame

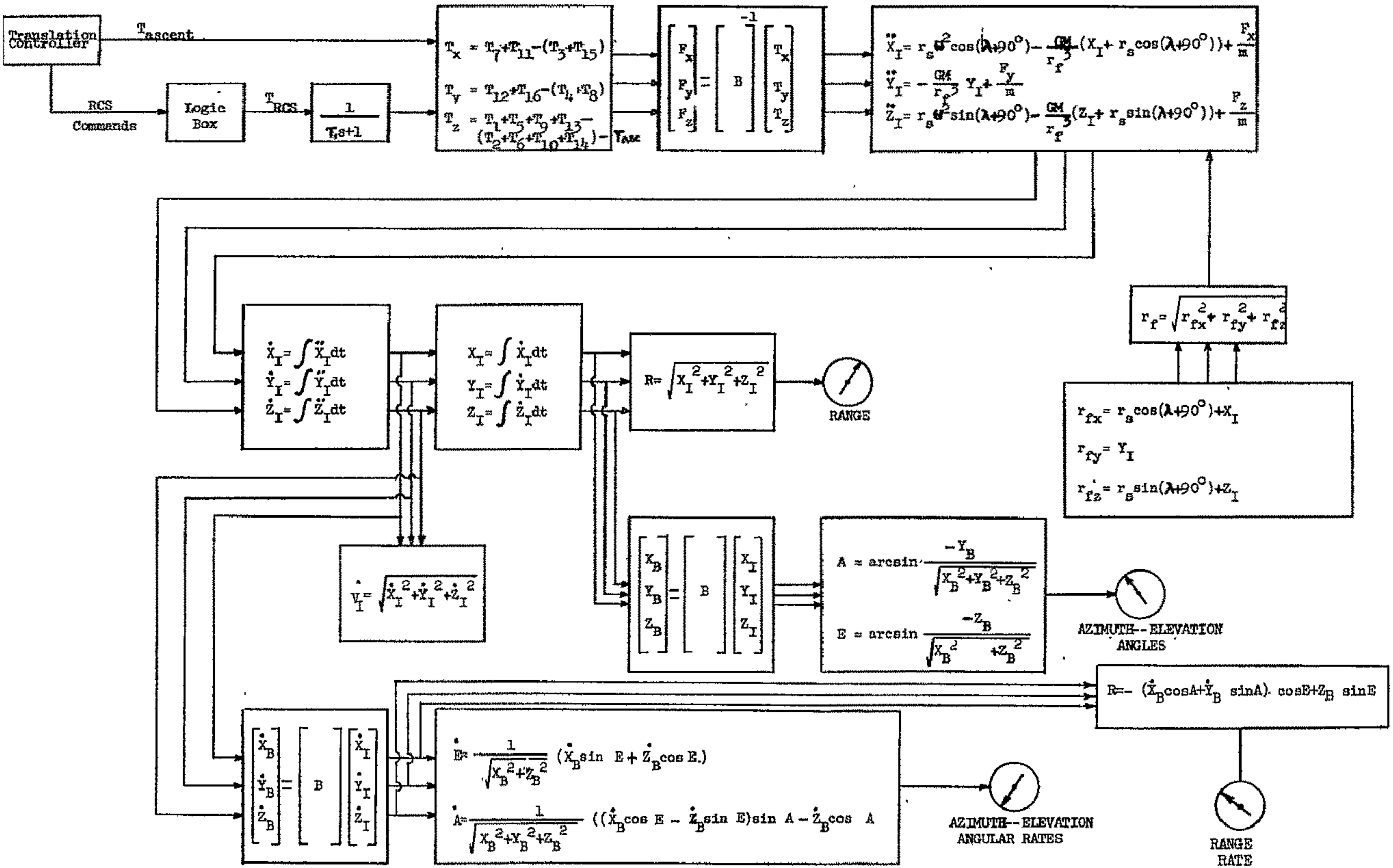

Figure 3 - Block Diagram of Translation Equations of Motion

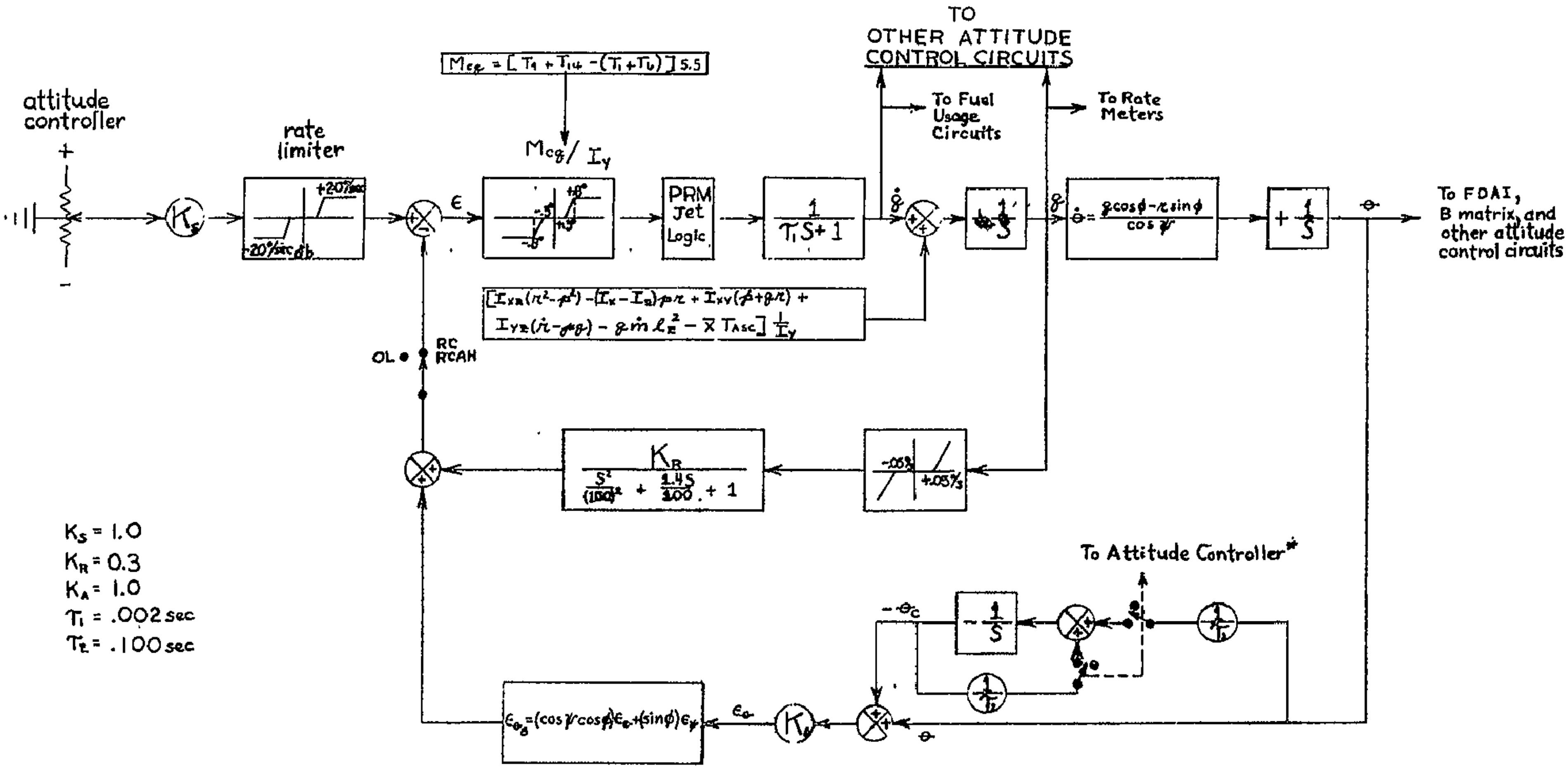

*All switches open when stick in deadzone. When stick is out of deadzone in any axis, the followup switches in all three axes shall close.

Figure 4 - Pitch Attitude Control Circuit

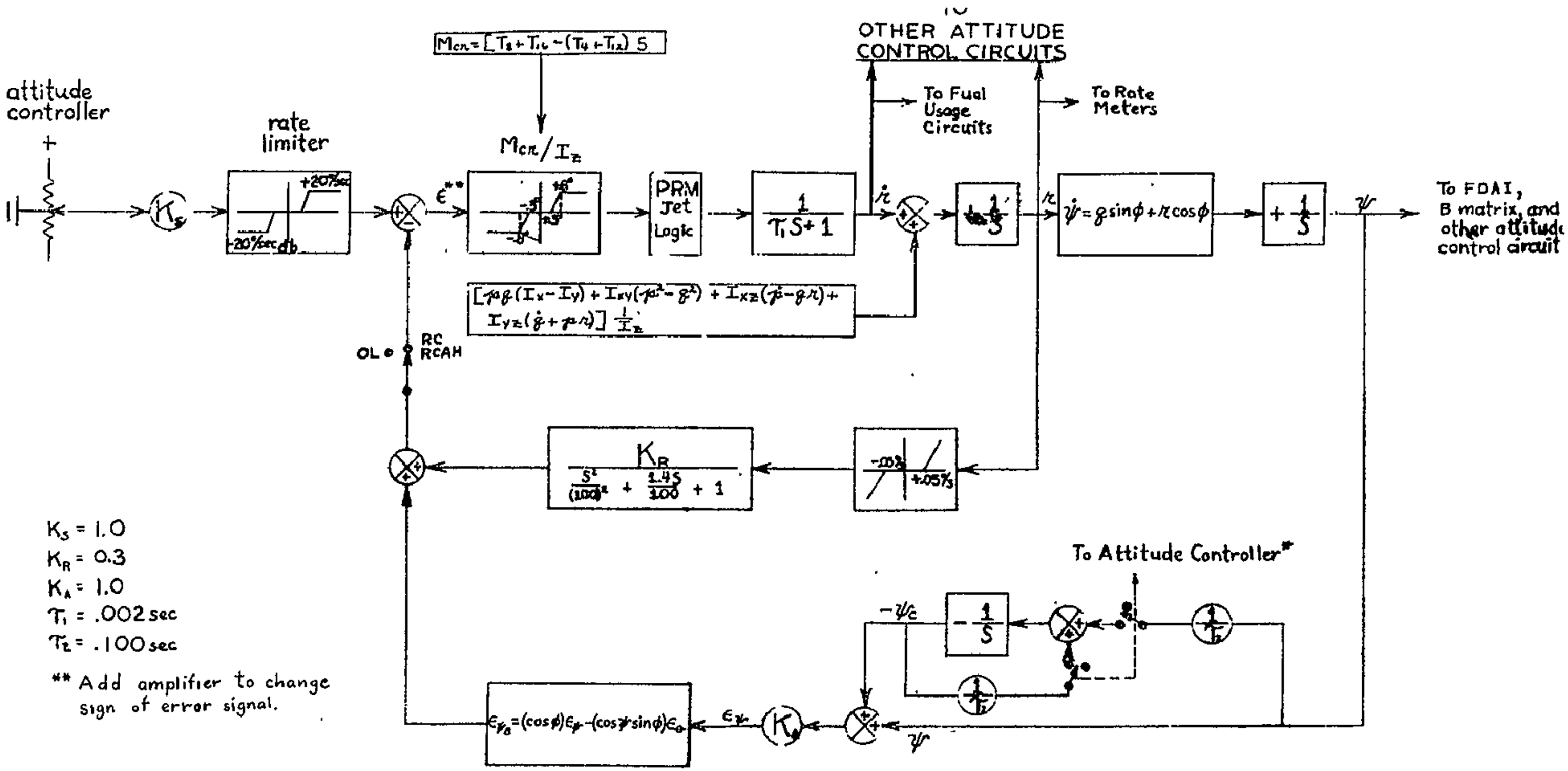

$K_S = 1.0$
$K_R = 0.3$
$K_A = 1.0$
$T_1 = .002$ sec
$T_2 = .100$ sec

** Add amplifier to change sign of error signal.

*All switches open when stick in deadzone. When stick is out of deadzone in any axis, the followup switches in all three axes shall close.

Figure 5 - Yaw Attitude Control Circuit

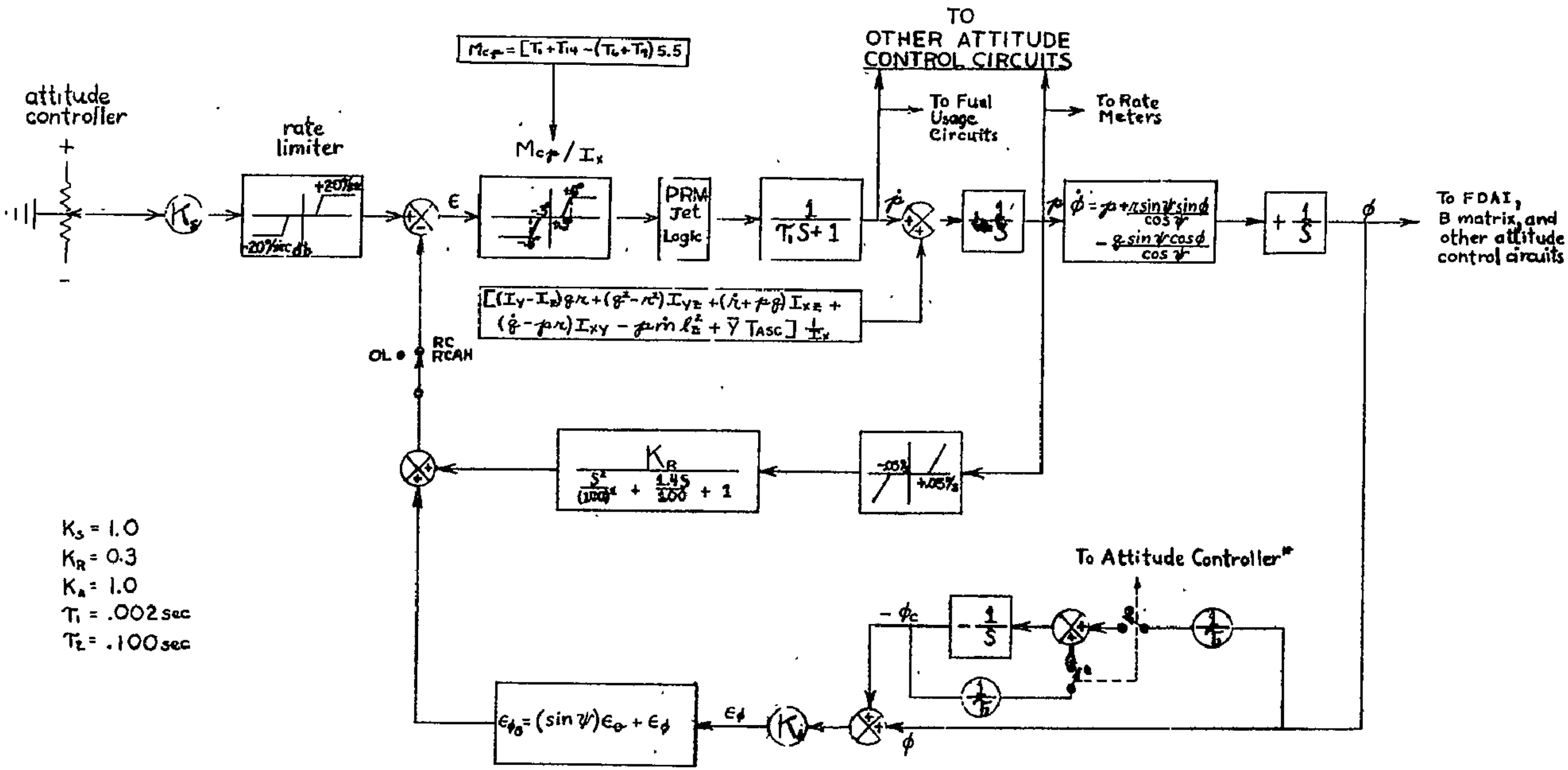

Figure 6 - Roll Attitude Control Circuit

*All switches open when stick in deadzone. When stick is out of deadzone in any axis, the followup switches in all three axes shall close.

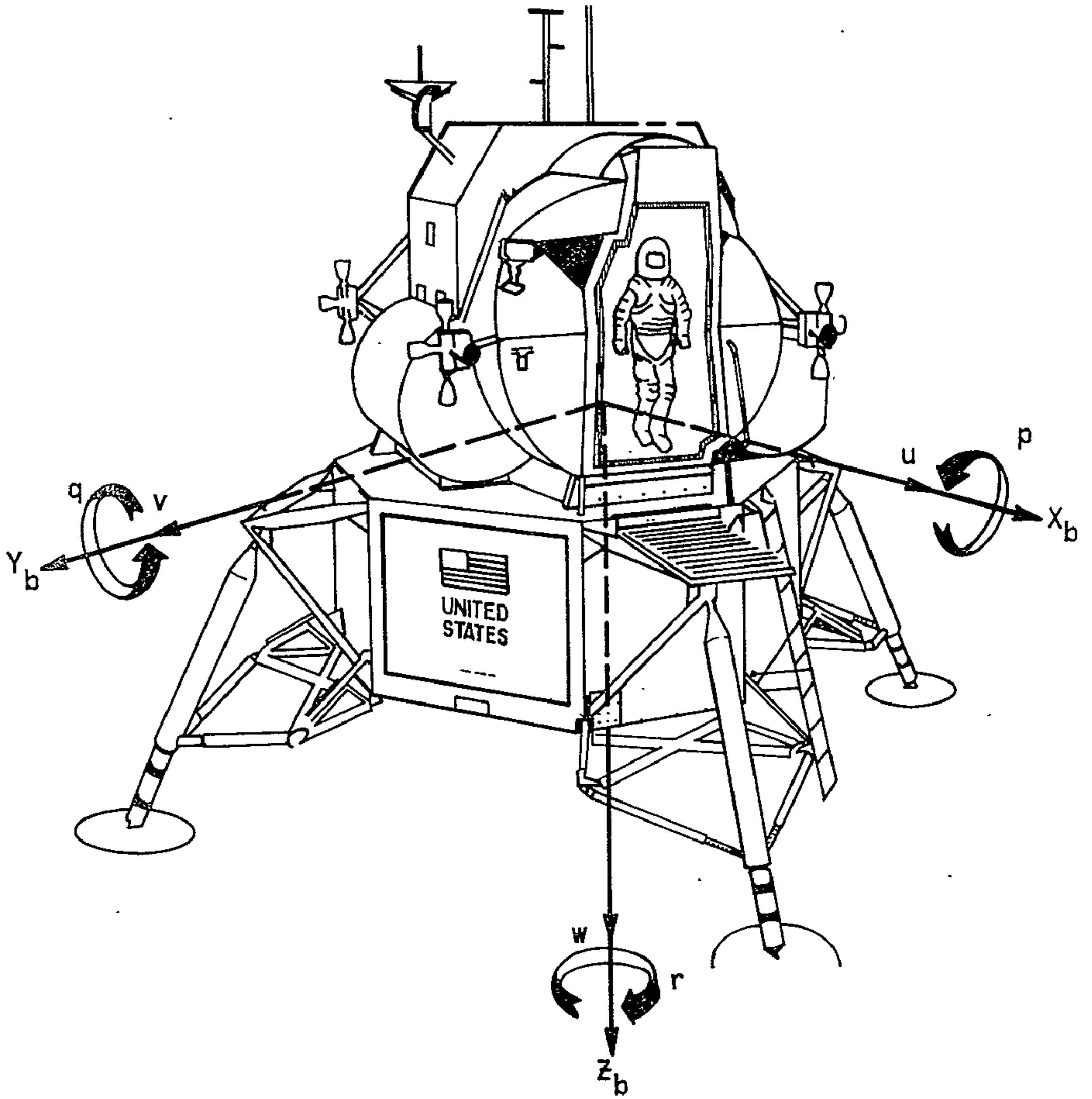

Figure 7 - General configuration of simulated vehicle.

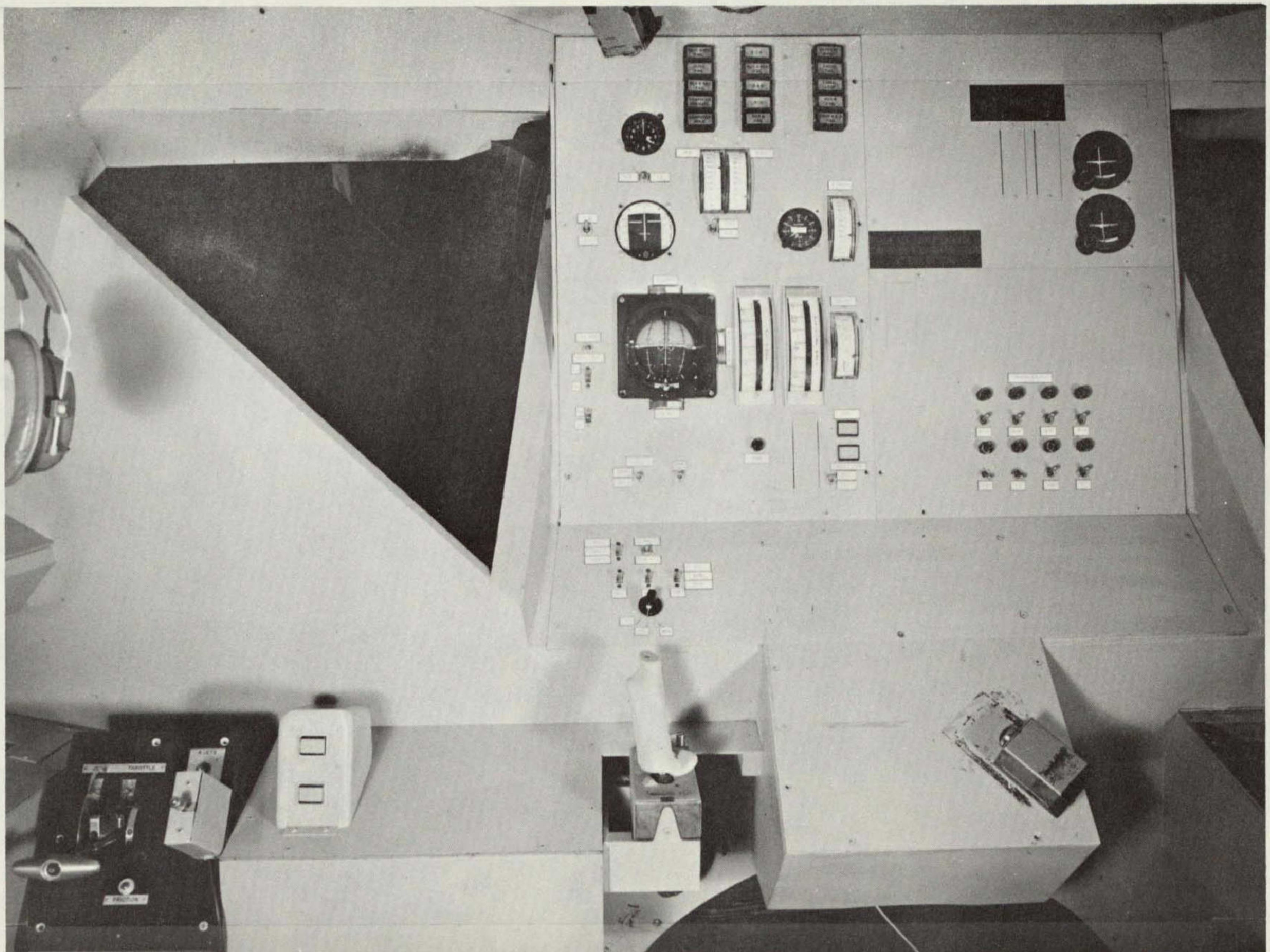

Figure 8a-Simulator Cockpit
Displays

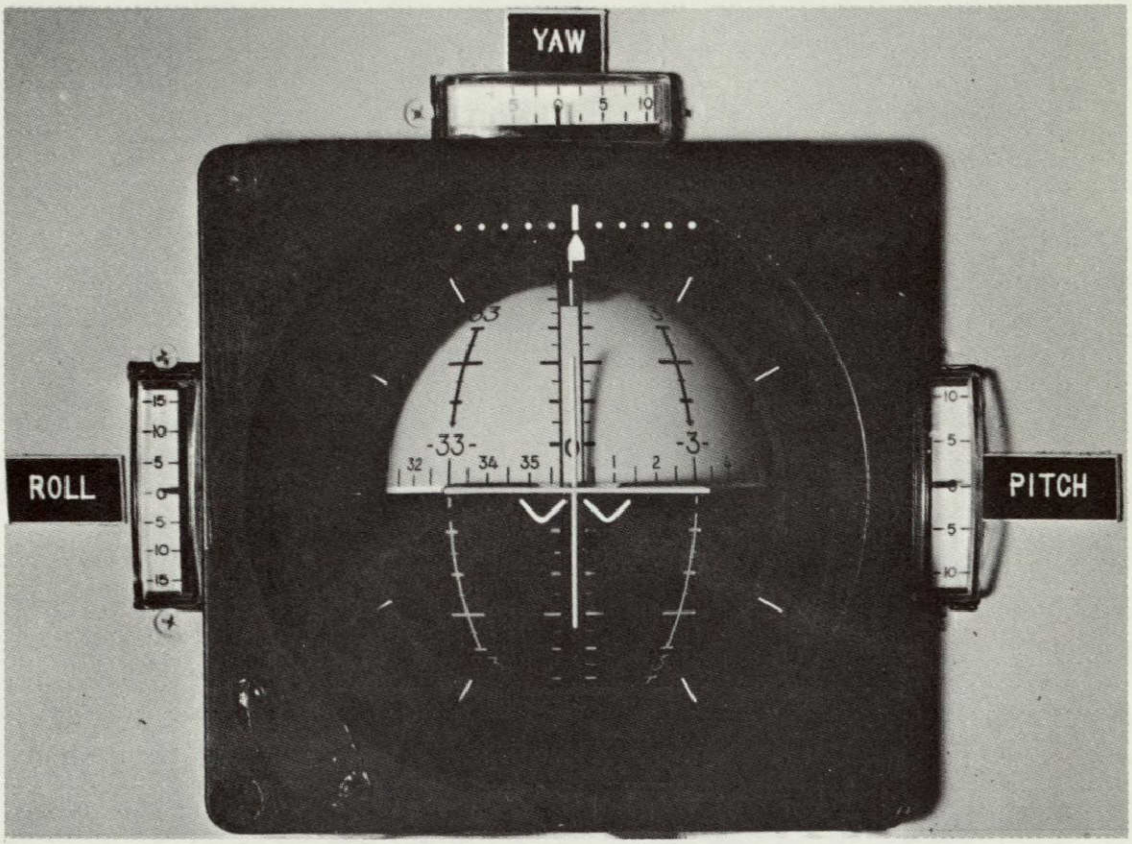

Figure 8b-Gemini FDAI (elevation and azimuth angles were displayed on error needles)

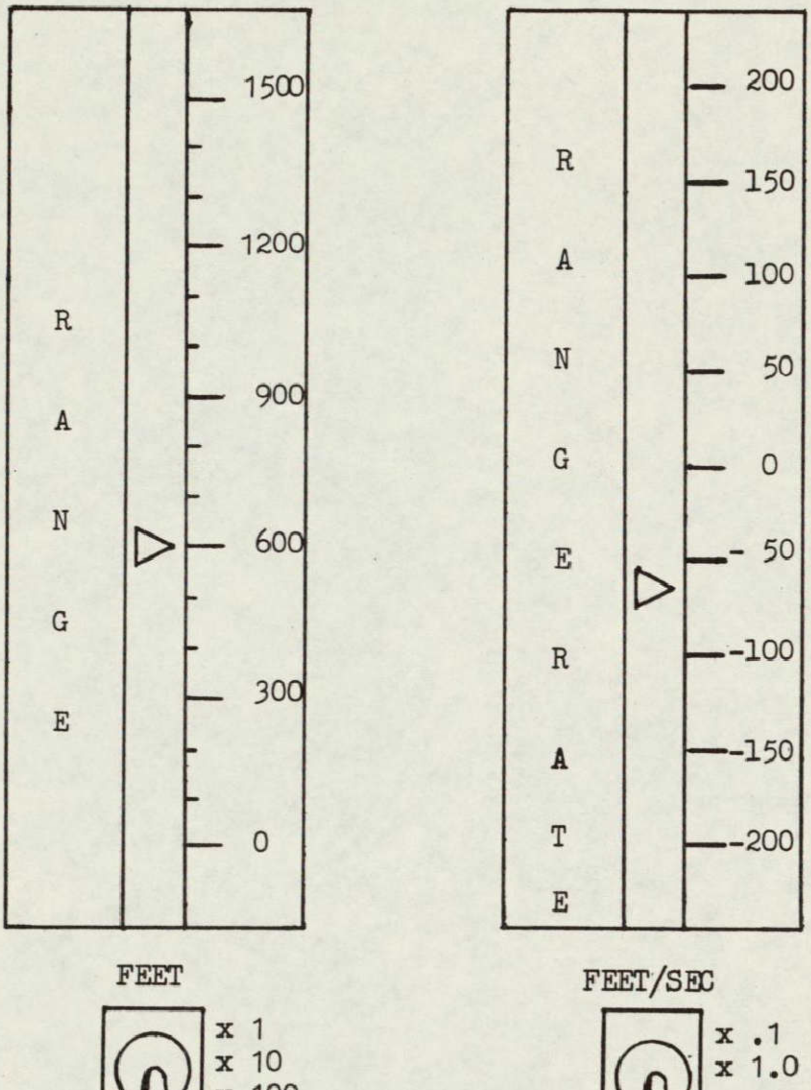

Figure 8c - Range and range-rate display

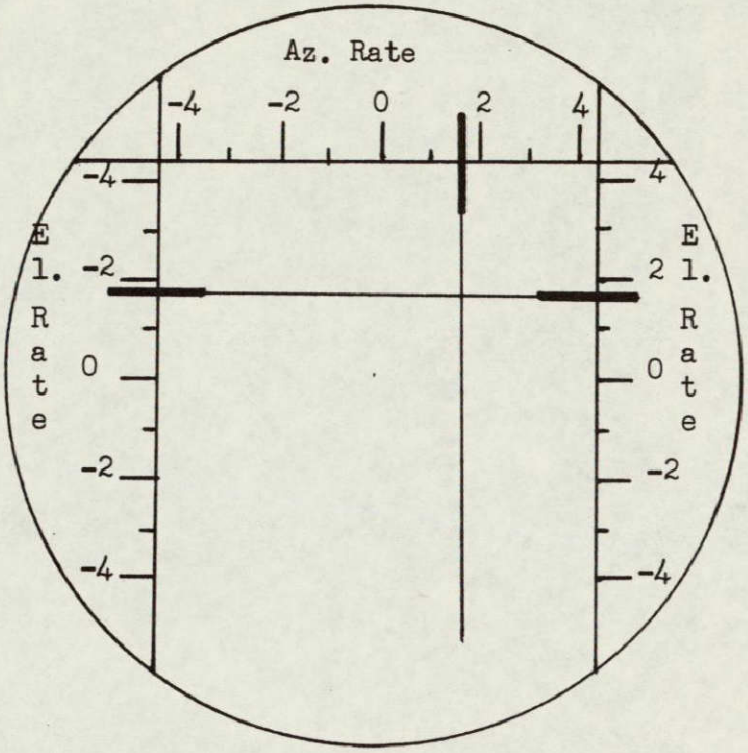

Note: Rates are milliradians per second.

Figure 8d - Azimuth rate and elevation rate display

NASA
S-63-8130

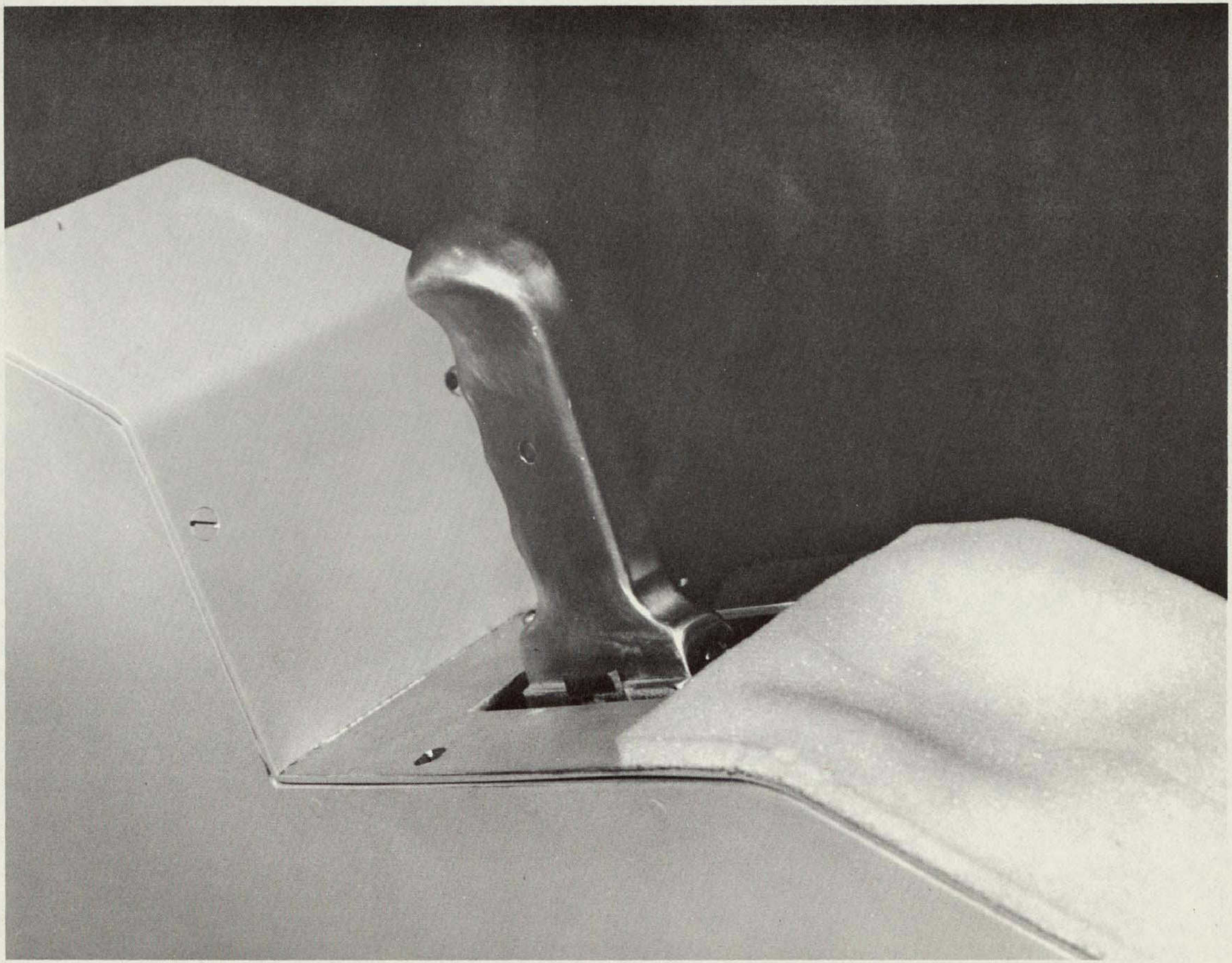

Figure 9 - Gemini Attitude Controller

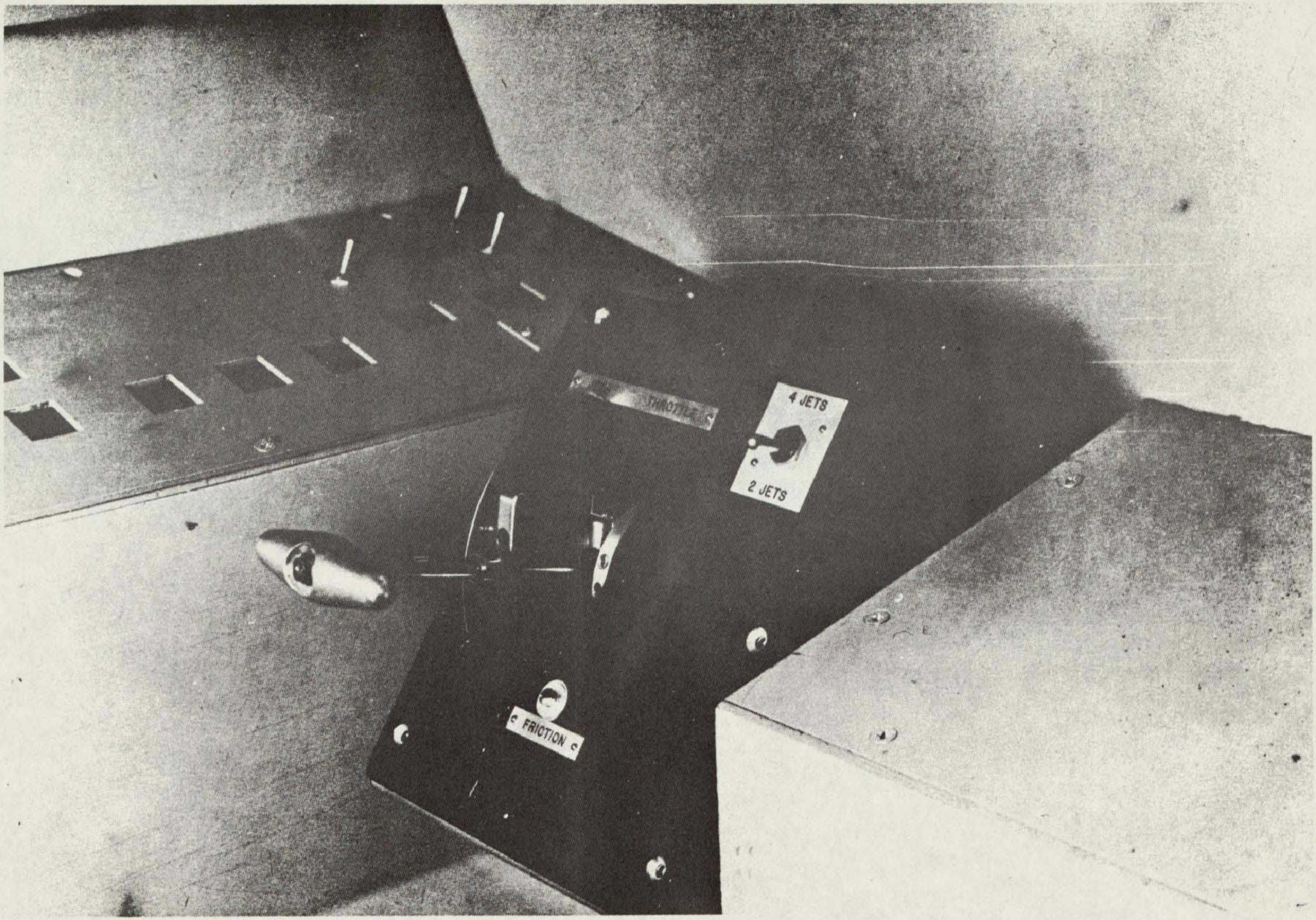

Figure 10 - LEM Translation Controller

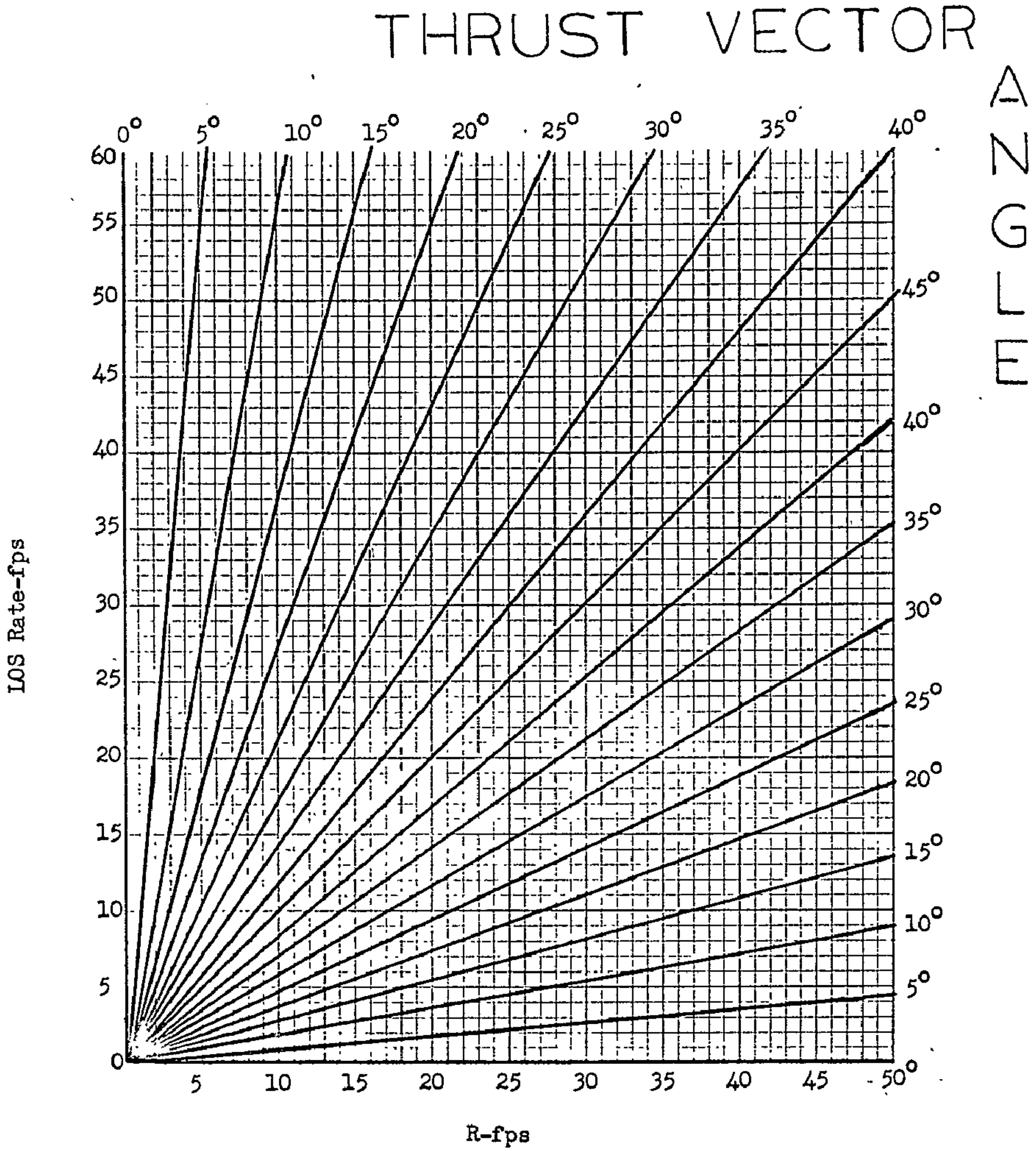

Figure 11.-Nomogram used to determine thrust vector angle for Technique No. 4

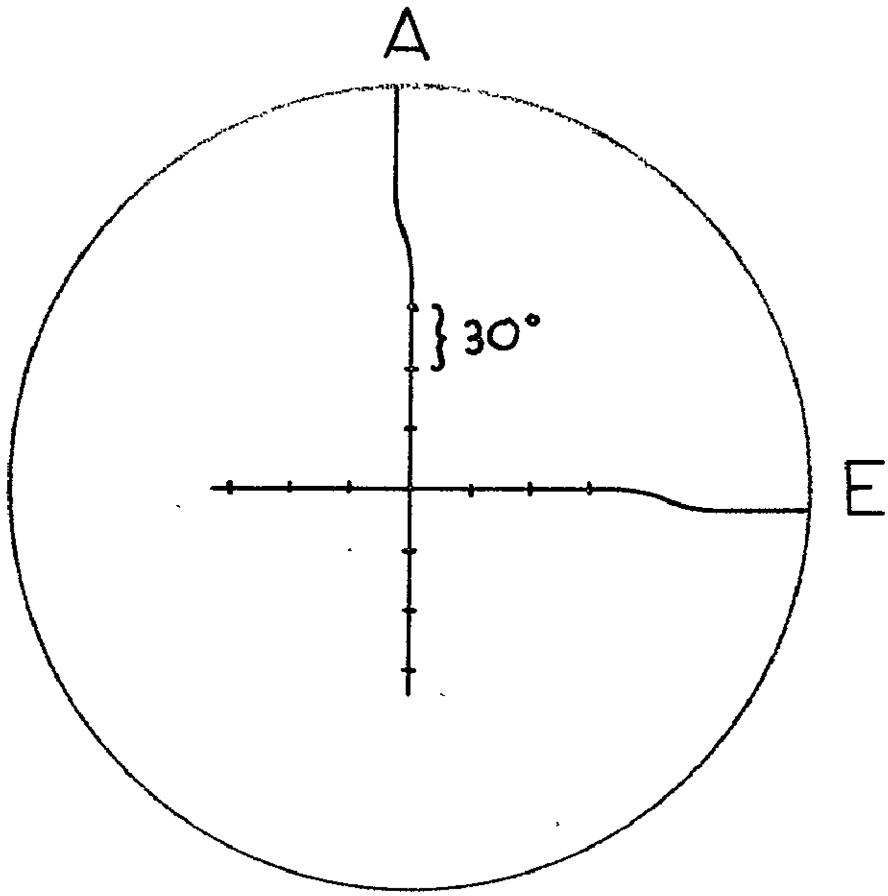

Figure 12.-Azimuth and elevation angle marks on FDAI error needles as used in this study

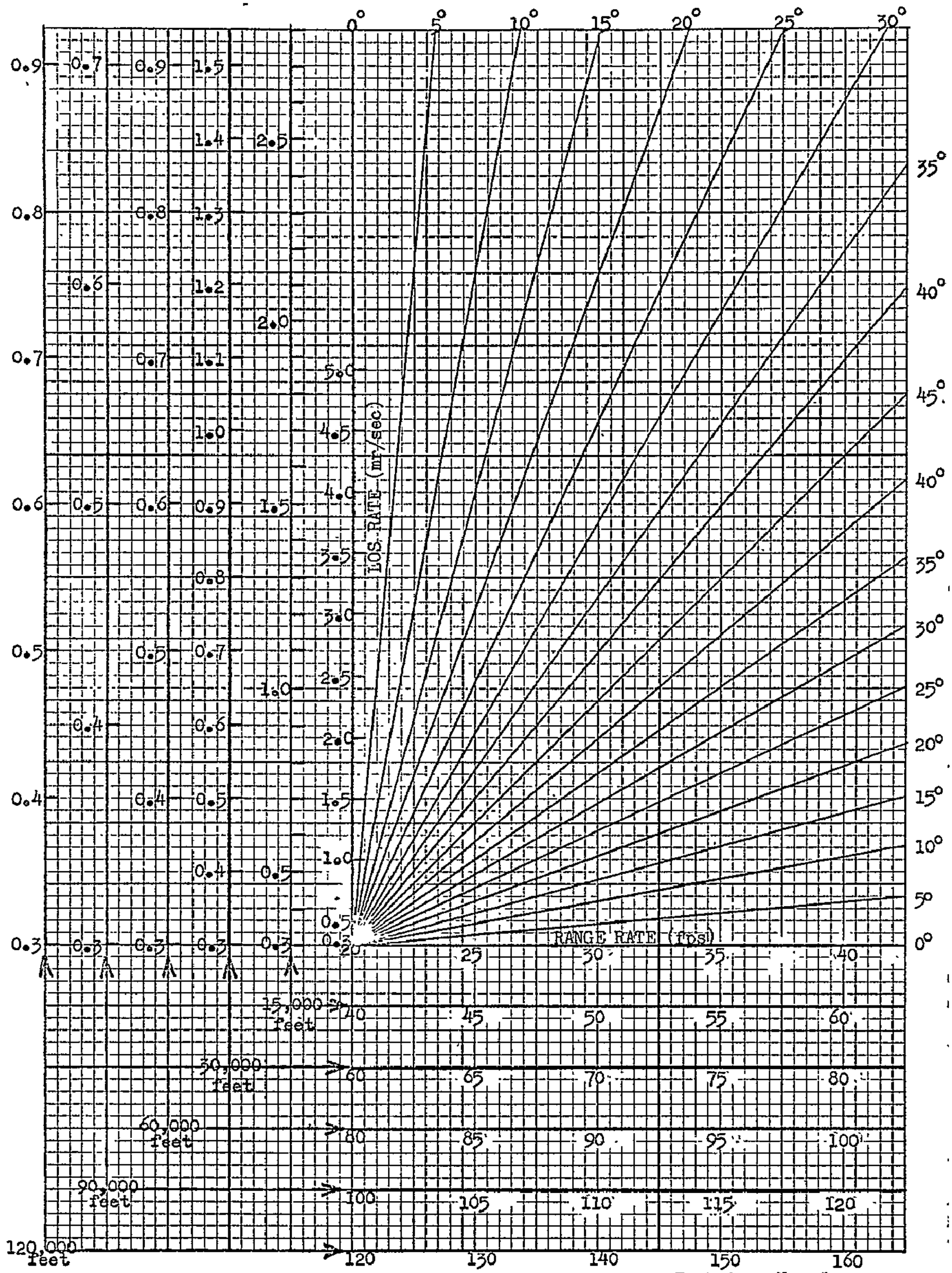

Figure 13-Nomogram used to determine thrust vector angle for Technique No. 5